

Kalman Linear Attention: Parallel Bayesian Filtering For Efficient Language Modelling and State Tracking

Vaisakh Shaj Cameron Barker Aidan Scannell Andras Szecsenyi Elliot J. Crowley Amos Storkey

University of Edinburgh

Abstract

State-space language models such as Mamba and gated linear attention (GLA) offer efficient alternatives to transformers due to their linear complexity and parallel training, but often lack the expressivity and robust state-tracking needed for complex reasoning. We address these limitations by reframing sequence modelling through a probabilistic lens, using Bayesian filters as a core primitive. While classical filters such as Kalman filters provide principled state estimation and uncertainty tracking, they are typically viewed as inherently sequential. We show that reparameterising the Kalman filter in information form enables its updates to be computed via an associative scan, allowing efficient parallel training. Building on this insight, we introduce the Kalman Linear Attention (KLA) layer, a neural sequence-modelling primitive that performs time-parallel probabilistic inference while maintaining explicit belief-state uncertainty. KLA offers strictly more expressive nonlinear updates and gating than GLA variants while retaining their computational advantages. On language modelling tasks, KLA matches or outperforms modern SSMs and GLAs across representative discrete token-manipulation and state-tracking benchmarks.

1. Introduction

Scaling sequence modelling beyond quadratic attention (Vaswani et al., 2017) is a central goal in large language and foundation model research. This has motivated interest in RNN-like architectures that support linear-time sequence modelling with efficient parallel training. Recent state-space models (SSMs), including S4/S5 (Gu et al., 2021; Smith et al., 2022), Mamba (Gu & Dao, 2023; Dao & Gu, 2024), and their

Correspondence to: Vaisakh Shaj <vaisakhs.shaj@gmail.com>.

Preprint. A version of this work was accepted and presented at the 1st Workshop on Epistemic Intelligence in Machine Learning (EIML) at EurIPS 2025.

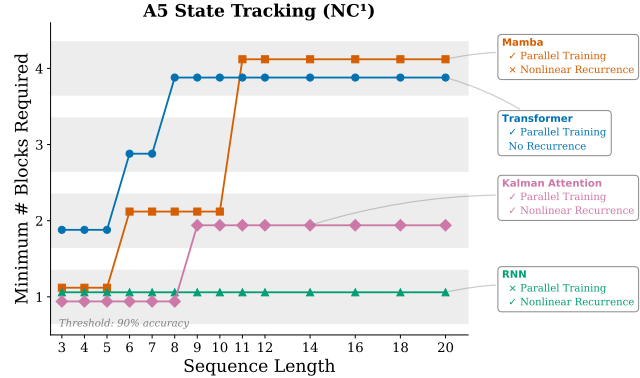


Figure 1. Minimum number of layers required to solve the A_5 (alternating group on 5 elements) permutation composition task (Merrill et al., 2024). KLA’s fractional linear updates fall between a fully nonlinear RNN and linear SSMs/transformers, requiring only 1 or 2 layers to solve the task without loss of parallelism.

successors, achieve this with $\mathcal{O}(\log T)$ depth, $\mathcal{O}(T)$ work, and linear or sublinear memory. This is essential for handling long contexts, on-device deployment and energy efficiency.

Despite their efficiency, adoption of SSMs is not as widespread as attention-based transformers. Recent work reinterprets modern SSMs and linear RNNs, including Mamba, as gated variants of linear attention (GLA) (Yang et al., 2023), where performance largely depends on how gates are defined. In all of these, the underlying hidden state updates are linear or affine, which limits their expressivity compared to softmax attention, whose normalisation induces nonlinear interactions between tokens. Furthermore, none of these represent state uncertainty explicitly. This contrasts with longstanding probabilistic linear state-space formalisms that lead to Kalman filter updates. These have both state uncertainty and nonlinear parameter updates.

In this paper, we ask: *Can we overcome the linear update constraints common to current GLA models to develop a state-space block that efficiently implements Kalman-like updates?*

We introduce **Kalman Linear Attention (KLA)**, which formulates sequence modelling as a Bayesian filtering

problem. KLA models two sources of uncertainty: process noise, which captures uncertainty in state evolution, and observation noise, which captures uncertainty in the information provided by each input token. Crucially, this uncertainty is not merely an output: it directly controls how new information is gated in state spaces.

At first glance, such Bayesian updates seem inherently sequential. Our key insight is that the information form of the Kalman filter admits a fractional-linear / Möbius associative structure that can be implemented using parallel scan-based algorithms, *despite its nonlinear update computation*. This allows Kalman-style updates to achieve the same $\mathcal{O}(\log T)$ parallel depth as models such as Mamba. The result is the **KLA** layer: a drop-in replacement for standard SSM or attention layers.

It is not enough to implement a new primitive without establishing that the extra expressiveness provides a benefit. We study the suitability of this continuous-state probabilistic model for discrete language modelling both theoretically and empirically, demonstrating important gains.

Contributions. Our contributions are as follows:

C1 Associative reparameterisation of Kalman filtering:

we reparameterise the diagonal linear–Gaussian filter in information form, showing the precision recursion is a Möbius (fractional-linear) map that composes associatively, enabling parallel prefix scans.

C2 Nonlinear gating from uncertainty: the precision-ratio gates are history-dependent and nonlinear, going beyond linear/affine SSM and gated linear attention updates while preserving linear-time scan structure.

C3 Kalman Linear Attention layer: we introduce KLA, a drop-in sequence mixer that can be integrated into modern language modelling pipelines and produces explicit belief-state uncertainty alongside representations.

C4 Scaling and accuracy: we provide scan-based implementations and show strong scaling with sequence length and competitive performance on synthetic LM tasks, long-context associative recall, and permutation-based state-tracking.

2. Related Work

Attention as filtering. The idea that intelligent systems must filter information has a long history that predates modern self-attention. In cognitive science, early theories of attention framed attention as a filtering mechanism that suppresses irrelevant signals and routes task-relevant signals under limited processing capacity (Broadbent, 1957;

	Softmax Attention	SSMs / GLA	KLA
Expressivity	Nonlinear	Linear	Fractional linear (Möbius)
Training efficiency	$\mathcal{O}(T^2)$	$\mathcal{O}(T)$	$\mathcal{O}(T)$
Inference efficiency	$\mathcal{O}(T)$	$\mathcal{O}(1)$	$\mathcal{O}(1)$
Seq-level uncertainty	✗	✗	✓
Parallel training	✓	✓	✓

Table 1. High-level comparison of sequence-mixing primitives. KLA combines the efficiency of SSMs with nonlinear (Möbius) updates and explicit belief-state uncertainty.

Treisman, 1969; Deutsch & Deutsch, 1963; Nielsen & Garcia, 2009). While early works strictly blocked signals, subsequent work softened this so that unattended streams are downweighted rather than eliminated (Treisman, 1969). Across these views, the core theme is that attention allocates scarce processing by selecting what matters in context.

In modern language models, transformer self-attention can be viewed as a form of context-based filtering (Vaswani et al., 2017). Tokens compete via similarity and the softmax suppresses most inputs whilst allowing a small subset to dominate the update. But this selection is *exemplar-based*: it requires retaining and comparing against all past keys/values, largely eliminating an explicit bottleneck and yielding $\mathcal{O}(T^2)$ cost at long context lengths.

Bayesian filtering and precision-control as attention.

Bayesian filters perform filtering as posterior inference under uncertainty. They update their prior beliefs with new observations, weighted through their precision (inverse variance). Intuitively, more reliable observations are given greater influence whilst unreliable evidence is downweighted. This yields a principled, interpretable gating mechanism where selection follows from uncertainty propagation.

Precision-weighted prediction errors have also been proposed as a computational account of attention in neuroscience and predictive coding (Rao & Ballard, 1999; Feldman & Friston, 2010). In this view, attention modulation is based upon confidence in sensory signals as opposed to deterministic reweighting. We adopt this view and show that Bayesian filters can be integrated into modern sequence modelling.

Temporal parallelisation of Bayesian filters. Särkkä & García-Fernández (2020) pioneered temporal parallelisation of Bayesian filtering and smoothing using prefix-sum algorithms, requiring specialised parameterisations to ensure associativity. To achieve associativity, they construct it by lifting each filtering step into a 5-tuple augmented representation, in the linear case. We show that no such augmentation is needed: Kalman updates in the information form are already Möbius maps, so precision composes by 2×2 matrix mul-

tiplication, a minimal, GPU-friendly structure (Theorems 1 and 2). Beyond parallelisation, we integrate these probabilistic primitives into learnable neural sequence models for language, where token-dependent observation likelihoods and dynamics are learned from data rather than specified a priori.

Deep Kalman filters and probabilistic state-space models.

Kalman filtering (Kalman, 1960) has a long history in reinforcement learning, control, and world modelling (Haarnoja et al., 2017; Watter et al., 2015; Hafner et al., 2019; 2020; Shaj Kumar et al., 2023). Deep Kalman filters embed linear-Gaussian state-space models (SSMs) inside neural networks and learn their parameters with either exact or variational inference (Krishnan et al., 2015; 2017; Karl et al., 2017; Fraccaro et al., 2016; Becker et al., 2019; Shaj et al., 2021). Although these approaches provide tractable inference, their recurrent update typically limits scalability to long contexts.

Recent deep RL work has paired deterministic SSM backbones (e.g., Mamba) with Kalman-style latent dynamics, using Särkkä’s temporal parallelisation to obtain variational posteriors (Becker et al., 2024), or replaced them entirely with parallelised Kalman layers to obtain uncertainty-aware representations under partial observability (Luis et al., 2024). In contrast, we adopt KLA as a standalone, closed-form probabilistic primitive for *language modelling*, competing directly with modern deterministic SSM/GLA mixers without requiring an additional deterministic SSM scaffold.

3. Background and Preliminaries

Modern language models can be abstracted as the composition of two functions: a shared representation (compression) map $f(\cdot; \theta)$ and a task-specific head g . Given a prompt $x_{1:T}$ of sequence length T , the backbone (the pretrained model) produces a compact latent representation $z_{1:T} = f(x_{1:T}; \theta)$ that captures structure in the language; the head then maps $z_{1:T}$ to outputs $y_{1:T}$ (e.g., next-token prediction, tagging, regression). Concrete parameterisations for f are chosen to balance expressivity with computational tractability. Transformers use softmax attention as the core primitive, whereas state-space models (SSMs) such as Mamba adopt structured recurrence with linear complexity.

Deterministic state-space models (SSMs) and Mamba.

Popular SSMs such as Mamba originate from structured state-space models (Gu et al., 2021). Building on their diagonal simplification (Gupta et al., 2022), a linear SSM maps a scalar input signal $x(t)$ to an output $y(t)$ through a latent state $h(t) \in \mathbb{R}^N$:

$$h'(t) = \mathbf{A}h(t) + \mathbf{B}x(t), \quad y(t) = \mathbf{C}h(t), \quad (1)$$

with $x(t), y(t) \in \mathbb{R}$, $\mathbf{A} = \text{diag}(a_1, \dots, a_N)$, $\mathbf{B} \in \mathbb{R}^{N \times 1}$, and $\mathbf{C} \in \mathbb{R}^N$. After discretisation, one processes a D -

dimensional sequence $\mathbf{X} \in \mathbb{R}^{T \times D}$ by running D independent copies of this recurrence, one per feature coordinate, or channel-, each with its own scalar input $x(t)$.

Mamba (S6) (Gu & Dao, 2023) makes this recurrence input-dependent (selective). For a single channel the update is

$$\mathbf{h}_t = \bar{\mathbf{a}}_t \odot \mathbf{h}_{t-1} + \bar{\mathbf{b}}_t x_t, \quad y_t = \mathbf{c}_t^\top \mathbf{h}_t, \quad (2)$$

where $x_t, y_t \in \mathbb{R}$, is system can be applied independently to each feature channel of a D -dimensional sequence $\mathbf{h}_t \in \mathbb{R}^N$ is the latent state, $\bar{\mathbf{a}}_t, \bar{\mathbf{b}}_t \in \mathbb{R}^N$ are discretised diagonal dynamics, and $\mathbf{c}_t \in \mathbb{R}^N$ is an input-dependent readout (the selective counterpart of \mathbf{C} in Equation (1)). The key property is *selectivity*: all parameters $(\bar{\mathbf{a}}_t, \bar{\mathbf{b}}_t, \mathbf{c}_t)$ are computed from the current input x_t , allowing the model to selectively filter which information to retain or discard at each step, while preserving linear-time scanning. This input-dependent gating can be seen as a learned form of filtering; in Section 3 we formalise this intuition through Bayesian filtering with explicit uncertainty.

State expansion. The dimension N in Equation (2) is a design choice known as *state expansion* (Gupta et al., 2022; Poli et al., 2024; Yu & Erichson, 2025). With $N=1$, each feature channel maintains a single scalar recurrence and the state is $\mathbf{h}_t \in \mathbb{R}^D$. Setting $N>1$ equips every channel with N parallel memory slots, expanding the state to $\mathbf{H}_t \in \mathbb{R}^{N \times D}$. Stacking the per-channel dynamics accordingly, we write $\bar{\mathbf{A}}_t, \bar{\mathbf{B}}_t \in \mathbb{R}^{N \times D}$ and $\mathbf{C}_t \in \mathbb{R}^{1 \times N}$. How the dynamics are allocated across these slots is itself an algorithmic decision: $\bar{\mathbf{A}}_t$ and $\bar{\mathbf{B}}_t$ may be *distinct* per slot or *shared* (tied) across channels, depending on the model variant. State expansion trades a larger memory footprint ($N \times D$ vs. D) for richer per-channel recurrence histories, as each slot can capture a different effective time-scale.

Attention from the SSM perspective. Ignoring scaling constants, auto-regressive softmax self-attention computes

$$\mathbf{Y} = \text{softmax}(\mathbf{Q}\mathbf{K}^\top + \mathbf{M})\mathbf{V}, \quad (3)$$

where $\mathbf{Q}, \mathbf{K}, \mathbf{V} = \mathbf{X}\mathbf{W}_q, \mathbf{X}\mathbf{W}_k, \mathbf{X}\mathbf{W}_v$ for $\mathbf{X}, \mathbf{Q}, \mathbf{K}, \mathbf{V} \in \mathbb{R}^{T \times D}$, $\mathbf{W}_q, \mathbf{W}_k, \mathbf{W}_v \in \mathbb{R}^{D \times D}$ and $\mathbf{M} \in (-\infty, 1)^{T \times T}$ is an auto-regressive mask.

Unlike the linear recurrence in Equation (2), softmax attention maintains a distinct memory of each \mathbf{K}_t and \mathbf{V}_t , yielding $\mathcal{O}(T^2)$ time and memory complexity.

By removing softmax we obtain Linear Attention $y_t = \mathbf{q}_t \sum_{i=0}^t \mathbf{k}_i^\top \mathbf{v}_i$ which permits an alternate recurrent form (Katharopoulos et al., 2020) that can be calculated in $\mathcal{O}(T)$ time and $\mathcal{O}(1)$ memory complexity, given by

$$\mathbf{H}_t = \mathbf{G}_t \odot \mathbf{H}_{t-1} + \mathbf{k}_t^\top \mathbf{v}_t \quad \text{and} \quad \mathbf{y}_t = \mathbf{q}_t \mathbf{H}_t. \quad (4)$$

where $\mathbf{G}_t \in \mathbb{R}^{N \times D}$ is an optional gating term.

Identifying $\mathbf{G}_t \equiv \bar{\mathbf{A}}_t$, $\mathbf{k}_t^\top \equiv \bar{\mathbf{B}}_t$ and $\mathbf{q}_t \equiv \mathbf{C}_t$ shows that GLA (Yang et al., 2023) matches Mamba when $\mathbf{W}_v = \mathbf{I}$.

Gaussian state-space models and Bayesian filtering. A classical probabilistic lens on sequential data is *state estimation*: we posit an (unobserved) latent state $\mathbf{z}_t \in \mathbb{R}^d$ that evolves over time, and assume the observed sequence $\mathbf{o}_t \in \mathbb{R}^p$ provides noisy evidence about that state. The goal of *Bayesian filtering* is to maintain the posterior belief $p(\mathbf{z}_t | \mathbf{o}_{1:t})$ online, recursively combining a *dynamics prior* (predict) with an *observation likelihood* (update).

When the dynamics and observations are linear with Gaussian noise, we obtain a linear–Gaussian state-space model:

$$\mathbf{z}_t = \mathbf{A}_t \mathbf{z}_{t-1} + \mathbf{w}_t, \quad \mathbf{w}_t \sim \mathcal{N}(\mathbf{0}, \mathbf{Q}_t), \quad (5)$$

$$\mathbf{o}_t = \mathbf{C}_t \mathbf{z}_t + \mathbf{v}_t, \quad \mathbf{v}_t \sim \mathcal{N}(\mathbf{0}, \mathbf{\Sigma}_t^{\text{obs}}), \quad (6)$$

in which the filtering posterior remains Gaussian, $p(\mathbf{z}_t | \mathbf{o}_{1:t}) = \mathcal{N}(\mu_t, \Sigma_t)$ and can be computed in closed form via the *Kalman filter* (KF), which is optimal in the minimum mean-squared error (MMSE) sense under these assumptions.

Control versus observation: two ways to read a token sequence. This filtering view contrasts with the common “controlled dynamics” interpretation of modern deterministic mixers (e.g., SSM/CDE-style models) (Muca Cirone et al., 2024), where the input sequence acts as an exogenous control that drives the hidden state forward. Bayesian filtering instead treats the sequence as noisy observations emitted by an underlying stochastic latent process. This single swap, control versus observation, changes what is conditioned on, what is random, and what computation is appropriate: forward simulation in the controlled view, versus posterior inference in the filtering view (see Figure 9 for a graphical comparison). Throughout this paper, we adopt the filtering perspective and show how it yields an attention-like sequence mixer with explicit uncertainty propagation.

Notational conventions. We index token sequences by $t \in \{1, \dots, T\}$. Bold uppercase terms denote matrices (or collections over time), lowercase denotes scalars, and boldface denotes vectors/sequences (e.g., \mathbf{x}_t). In the diagonal (per-coordinate) parameterisation, we identify diagonal matrices with their diagonal terms and apply scalar recursions elementwise. An overbar denotes the discretised counterpart of a continuous-time parameter, e.g. \bar{a}_t is obtained by discretising a continuous-time decay parameter.

For completeness, Appendix C includes additional background material on related mathematical constructs such as Möbius (Fractional Linear) Transforms, the Information Form of Gaussian distributions, and Information Filters.

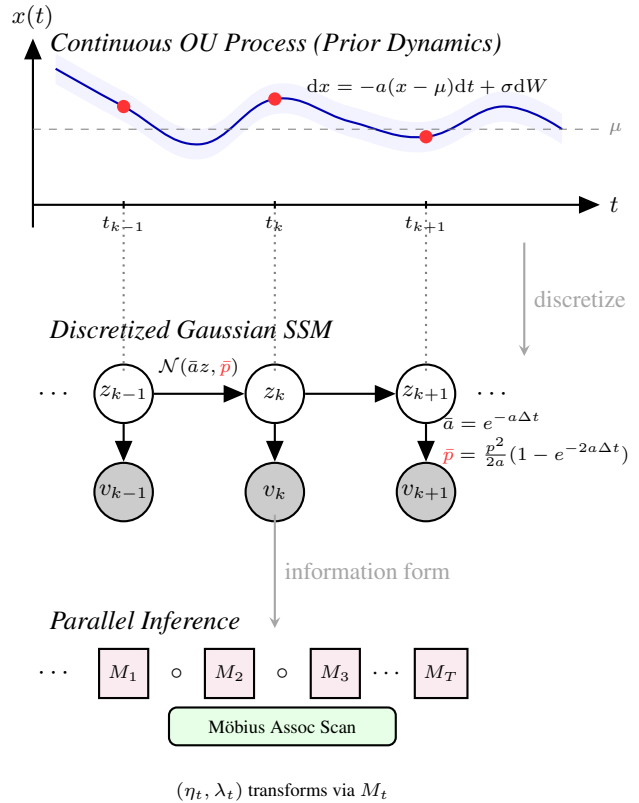


Figure 2. From OU dynamics to parallel inference. **(Top)** Continuous-time OU prior. **(Middle)** Discrete linear-Gaussian SSM. **(Bottom)** Möbius scan for parallel posterior state estimation.

4. Method

We introduce *Kalman Linear Attention (KLA)* as a *probabilistic* sequence mixer. Instead of deterministically updating a hidden state as in modern SSM mixers, KLA maintains a belief state over a latent representation, consisting of a posterior mean and an explicit uncertainty (precision/covariance). This probabilistic view turns sequence mixing into state estimation from noisy token evidence, and provides a principled mechanism for adaptivity and a gating mechanism derived from relative uncertainties of state and observation.

Our method is organised around two ideas. **(i) A probabilistic SSM view of sequence mixing.** We cast token processing as inference in a linear–Gaussian state-space model. Each token contributes a (noisy) observation v_t of the latent state through an observation operator k_t , while the latent evolves under a continuous-time stochastic prior that we discretise for sequences.

(ii) Parallelisable filtering via information form. We address the main obstacle to using Bayesian filters as sequence mixers: classical filtering is recursive and appears inherently sequential. We show that by working in *information form* (precisions and natural parameters), the posterior updates acquire a parallelisation-friendly Möbius (fractional-linear)

structure. This yields a scalable implementation of Bayesian sequence mixing with the computational profile of modern linear-time mixers, while preserving clear probabilistic semantics.

Throughout this section, [blue terms](#) denote uncertainty-aware quantities absent in deterministic SSMs.

4.1. Stochastic Dynamics and Token Likelihood

Dynamics prior (predict step) via OU discretisation. Modern SSM mixers ([Gu et al., 2021](#); [Smith et al., 2022](#)) are often motivated from continuous-time dynamics and then discretised to operate on token sequences. In this view, a simple linear ODE yields a discrete-time recurrence in which the discretised decay \bar{a}_t acts as a forget factor, and the step size Δt controls the effective time scale. This provides an appealing interpretation of SSM channels as a spectrum of memories parameterised by their decay rates.

KLA adopts the same continuous-to-discrete modelling pipeline, but makes one conceptual change: we treat latent evolution as inherently uncertain. Concretely, we specify a continuous-time *stochastic* dynamics prior and discretise it exactly. We use an Ornstein–Uhlenbeck (OU) process as the prior because it is the canonical mean-reverting diffusion (and the continuous-time analogue of a stable AR(1)): it preserves exponential forgetting while introducing an explicit process-noise term that captures unmodelled variability and uncertainty in the latent dynamics. Under exact discretisation, the OU prior induces a Gaussian transition

$$\mathbf{z}_t \mid \mathbf{z}_{t-1} \sim \mathcal{N}(\bar{\mathbf{a}}_t \odot \mathbf{z}_{t-1}, \bar{\mathbf{p}}_t), \quad (7)$$

$$\bar{\mathbf{a}}_t = e^{-\mathbf{a}\Delta t}, \quad \bar{\mathbf{p}}_t = \frac{\mathbf{p}^2}{2\mathbf{a}} \odot (1 - e^{-2\mathbf{a}\Delta t}), \quad (8)$$

where $\bar{\mathbf{a}}_t$ denotes the decay and $\bar{\mathbf{p}}_t$ the process-noise variance.

Multi-channel specialisation. Importantly, $\bar{\mathbf{p}}_t$ is coupled to $\bar{\mathbf{a}}_t$ by construction: the same decay and time-scale parameters \mathbf{a} that control decay also determine how uncertainty accumulates between observations. This yields per-channel specialisation along two linked axes: memory decay and drift. Different coordinates can learn different decay rates (short- vs. long-memory channels), and their process noise $\bar{\mathbf{p}}_t$ sets how freely each channel can drift away from its predicted trajectory between tokens. This is different from Mamba, where the timescale/discretisation parameter is token-dependent and undertakes the role of selection/filtering at each timestep, whereas in our case selection/filtering is achieved purely via uncertainties without overloading Δ_t with additional roles.

Input token likelihood as noisy evidence (update step).

To connect this dynamics prior to input token sequences, we model each token as providing noisy evidence about the

Attention	Deterministic SSM / KLA (probabilistic GLA)
Query operator \mathbf{q}_t	Output/readout map \mathbf{C}_t
Key operator \mathbf{k}_t	Input to latent map \mathbf{b}_t
Value \mathbf{v}_t	Token input/control \mathbf{u}_t
Output \mathbf{y}_t	Output \mathbf{y}_t
<i>Hidden state (implicit in attention, explicit in SSMs/KLA):</i>	
—	Hidden state \mathbf{h}_t
—	Posterior belief $\mathcal{N}(\boldsymbol{\mu}_t, \boldsymbol{\Lambda}_t^{-1})$ over \mathbf{z}_t
—	State decay $\bar{\mathbf{a}}_t = e^{-\mathbf{a}(t)\Delta t}$
—	State decay $\bar{\mathbf{a}}_t = e^{-\mathbf{a}\Delta t}$
<i>Uncertainty terms (explicit in KLA only):</i>	
—	Value precision $\boldsymbol{\Lambda}_t^v$
—	State precision $\boldsymbol{\lambda}_t$
—	Process noise $\bar{\mathbf{p}}_t = \frac{\mathbf{p}^2}{2\mathbf{a}} \odot (1 - e^{-2\mathbf{a}\Delta t})$

Table 2. Notation alignment across attention, SSMs, and KLA. Precisions ($\boldsymbol{\lambda}$, $\boldsymbol{\Lambda}^v$, $\boldsymbol{\Lambda}^p$) are inverse variances encoding confidence: higher precision means lower uncertainty.

latent state:

$$\mathbf{v}_t \mid \mathbf{z}_t \sim \mathcal{N}(\mathbf{k}_t \odot \mathbf{z}_t, (\boldsymbol{\Lambda}_t^v)^{-1}), \quad (9)$$

where \mathbf{v}_t is token-derived content, \mathbf{k}_t is an observation operator, and $\boldsymbol{\Lambda}_t^v$ is the value precision representing confidence in the token evidence. Combining Equation (7) with Equation (9) yields a linear–Gaussian state-space model, and *sequence mixing corresponds to posterior inference* of the latent state given token evidence.

Output readout as a query/task-conditioned projection of the belief state. So far, $(\mathbf{k}_t, \mathbf{v}_t, \boldsymbol{\Lambda}_t^v)$ define how input token evidence updates the latent belief $p(\mathbf{z}_t \mid \mathbf{v}_{1:t})$. A remaining design choice is how to use this belief to produce an output representation for downstream prediction. Deterministic SSM mixers typically apply a readout $\mathbf{y}_t = \mathbf{C}_t \odot \mathbf{h}_t$, while transformers use a query to determine what information should be extracted from stored context. KLA adopts an analogous view: the *query* \mathbf{q}_t specifies *what we want to read out* from the inferred belief state at time t . To make this explicit, we introduce a (linear–Gaussian) readout model

$$\mathbf{y}_t \mid \mathbf{z}_t \sim \mathcal{N}(\mathbf{q}_t \odot \mathbf{z}_t, (\boldsymbol{\Lambda}_t^{\text{out}})^{-1}), \quad (10)$$

where $\boldsymbol{\Lambda}_t^{\text{out}}$ is an *output precision* (readout noise). In this work we take the deterministic-readout limit $\boldsymbol{\Lambda}_t^{\text{out}} \rightarrow \infty$ (equivalently, zero readout noise), so that the output is the posterior mean projection

$$\mathbf{y}_t = \mathbf{q}_t \odot \boldsymbol{\mu}_t, \quad (11)$$

which mirrors the role of a query-conditioned readout in attention and a C_t -projection in SSMs. An intuitive analogy is accumulating beliefs over time via posterior inference through an input modality v_t (say image sensors) via observation model k_t and converting the latent beliefs to an output modality (say proprioceptive sensors) y_t via query model q_t .

Gaussian SSM view of q - k - v interactions. We can summarise the attention-aligned probabilistic interpretation as a linear-Gaussian state-space model in which keys and values parameterise the *likelihood* (token evidence), while queries parameterise a *readout* applied after inference. Let z_t denote the latent state and let (k_t, v_t, Λ_t^v) be token-dependent likelihood parameters produced from the input sequence. The generative model is:

$$\text{Prior} \quad z_t \mid z_{t-1} \sim \mathcal{N}(\bar{a}_t \odot z_{t-1}, \bar{p}_t), \quad (12)$$

$$\text{Evidence} \quad v_t \mid z_t \sim \mathcal{N}(k_t \odot z_t, (\Lambda_t^v)^{-1}), \quad (13)$$

$$\text{Readout} \quad y_t \mid z_t \sim \mathcal{N}(q_t \odot z_t, (\Lambda_t^{\text{out}})^{-1}). \quad (14)$$

In this view, k_t specifies the observation geometry (how token evidence constrains the latent), v_t is the observed token evidence, and Λ_t^v is its reliability (precision). The query q_t instead specifies what component of the inferred latent state is exposed as the output.

4.2. Parallel Inference via Möbius and Affine Scans

A major obstacle to using Bayesian filters as sequence mixers is that classical filtering is *recursive* and thus appears inherently sequential. Our key observation is that, in *information form*, the updates admit a *compositional* structure that can be implemented with parallel scans.

Information form. We represent the Gaussian posterior by its precision and natural (canonical) parameter:

$$p(z_t \mid v_{1:t}) = \mathcal{N}(\mu_t, \lambda_t^{-1}), \quad \eta_t := \lambda_t \odot \mu_t. \quad (15)$$

This parameterisation is convenient because, in linear-Gaussian models, incorporating token evidence corresponds to *adding* canonical parameters (precisions and information means), while the remaining “predict” transformation induced by the dynamics takes a structured form. As we show next, these structured updates *compose associatively* across time, which is exactly what enables parallel prefix scans.

Theorem 1 (Precision Update as a Möbius Transformation). *Let λ_t be the posterior precision at time t in the diagonal linear-Gaussian model Equation (7)–Equation (9). Define $\phi_t := k_t^2 \odot \Lambda_t^v$. Then the map $\lambda_{t-1} \mapsto \lambda_t$ is a linear-*

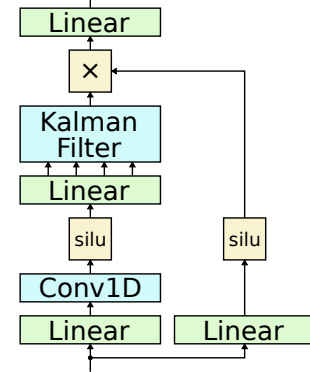


Figure 3. **Block architecture.** The block follows the fused-MLP design of Mamba, with the Kalman Filter as a drop-in replacement for any SSM/Attention primitive.

fractional (Möbius) transform:

$$\lambda_t = \mathbf{M}_t(\lambda_{t-1}) = \frac{\alpha_t \odot \lambda_{t-1} + \beta_t}{\gamma_t \odot \lambda_{t-1} + \delta_t}, \quad (16)$$

$$\mathbf{M}_t = \begin{pmatrix} \alpha_t & \beta_t \\ \gamma_t & \delta_t \end{pmatrix} = \begin{pmatrix} 1 + \bar{p}_t \odot \phi_t & \bar{a}_t^2 \odot \phi_t \\ \bar{p}_t & \bar{a}_t^2 \end{pmatrix}. \quad (17)$$

Interpretation: precision track as uncertainty-driven gating. While Equation (16) is nonlinear in λ_{t-1} , it admits a simple “gate-like” rearrangement:

$$\lambda_t = \underbrace{(\bar{a}_t^2 + \bar{p}_t \odot \lambda_{t-1})^{-1} \odot \lambda_{t-1}}_{\text{(confidence history)}} + \underbrace{\phi_t = k_t^2 \odot \Lambda_t^v}_{\text{(confidence in current token)}}. \quad (18)$$

The shared denominator $\bar{a}_t^2 + \bar{p}_t \odot \lambda_{t-1}$ introduces *history dependence*: as accumulated precision grows, the model naturally becomes more selective about incorporating new evidence. This “precision track” will later induce input/forget-gate behaviour for the mean update (Equation (19)).

Corollary 1 (Precision Updates via Parallel Prefix Scan). *Given λ_0 and matrices $\{\mathbf{M}_t\}_{t=1}^T$ from Theorem 1, the posterior precisions $\{\lambda_t\}_{t=1}^T$ can be computed by a parallel prefix scan over $\{\mathbf{M}_t\}$ with $\mathcal{O}(T)$ work and $\mathcal{O}(\log T)$ depth.*

Theorem 2 (Mean Update as Affine Transformations). *Let $\eta_t := \lambda_t \odot \mu_t$ be the posterior information mean and Λ_t^v the value precision. Given the precision path $\{\lambda_t\}$, the information mean evolves affinely:*

$$\eta_t = \underbrace{(\bar{a}_t^2 + \bar{p}_t \odot \lambda_{t-1})^{-1} \odot \bar{a}_t}_{f_t \text{ (history-dependent forget gate)}} \odot \eta_{t-1} + \underbrace{k_t \odot \Lambda_t^v \odot v_t}_{\text{token evidence}}. \quad (19)$$

Corollary 2 (Mean Updates via Parallel Prefix Scan). *The posterior information means $\{\eta_t\}_{t=1}^T$ are computable via parallel prefix scan over the affine transformations in Theorem 2 in $\mathcal{O}(T)$ work and $\mathcal{O}(\log T)$ depth.*

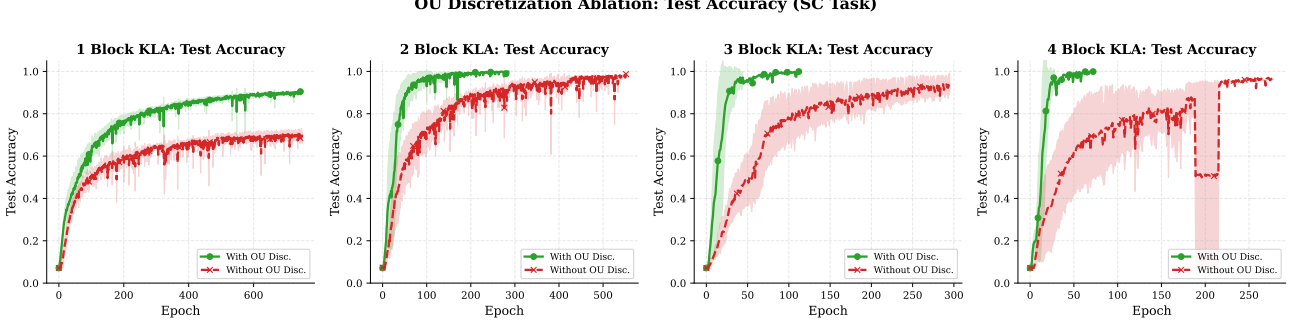


Figure 4. Ablation of OU prior dynamics and discretisation (Section 4.1) on Selective Copy ($T = 256$). OU discretisation improves accuracy and learning stability, especially for deeper models.

Special cases: Under deterministic ($\mathbf{p}_t = 0$) and linear time-invariant (LTI) settings, the KLA updates reduce to convolutions computable in $\mathcal{O}(\log T)$ time via FFT (see Theorem 3 in the Appendix).

4.3. KLA as a Drop-in Probabilistic Sequence Mixer

In order to instantiate the above parallel Bayesian filter as a neural network layer, we parametrise the observation value and precision ($\mathbf{v}_t, \Lambda_t^V$) as well as the observation and read-out operators ($\mathbf{k}_t, \mathbf{q}_t$) in terms of the layer input sequence $x_{1:T}$. The observation variance is parametrised such that it is positive. For the continuous stochastic prior (Section 4.1), we treat \mathbf{a}_t and \mathbf{p}_t as learnable, time-invariant parameters \mathbf{a} and \mathbf{p} , respectively, in contrast to Mamba where \mathbf{a}_t is token-dependent and time-varying.

The block architecture follows a fused MLP architecture as shown in Figure 3. Following the Mamba design, we employ standard scaffolding components paired with the KLA sequence mixer: a 1D causal convolution with kernel size 4 and SiLU activation, along with residual connections and simple nonlinearities. Figure 8 and Appendix A for more architecture and implementation details. We implement efficient Triton (Tillet et al., 2019) kernels for the Linear and Möbius parallel scan primitives; however, we do not fuse the whole block into a single kernel, which has been shown to be necessary in order to minimise memory movement and achieve peak performance in other SSMs, especially for the backward pass. Additionally, the KLA posterior mean recurrence can be unrolled into an equivalent matrix multiplication with a lower-triangular ‘‘attention’’ matrix; we visualise this structure in Figure 12 (Appendix E).

4.4. Training Loss

We consider two training losses:

(i) Posterior mean: logits $\ell_t = g_\theta(\mathbf{y}_t)$ are obtained from the posterior-mean readout $\mathbf{y}_t = \mathbf{q}_t \odot \boldsymbol{\mu}_t$ and trained with cross-entropy,

(ii) Log marginal likelihood: minimises the negative log marginal likelihood of the output token o_t ,

$$\begin{aligned} -\log p_\theta(o_t \mid \mathbf{X}) &= -\log \int \underbrace{p_\theta(o_t \mid \mathbf{y}_t)}_{\text{decoder}} \underbrace{p_\theta(\mathbf{z}_t \mid \mathbf{X})}_{\text{KLA posterior}} d\mathbf{z}_t \\ &\approx -\log \left(\frac{1}{S} \sum_{s=1}^S p_\theta(o_t \mid \mathbf{y}_t^{(s)}) \right), \quad (20) \end{aligned}$$

with $\mathbf{z}_t^{(s)} \sim p_\theta(\mathbf{z}_t \mid \mathbf{X})$ and $\mathbf{y}_t^{(s)} = \mathbf{q}_t \odot \mathbf{z}_t^{(s)}$. More details on the loss functions used are given in Appendix A.

5. Experiments

We evaluate KLA as a *drop-in sequence mixer* for language modelling. Although KLA is derived from continuous-time Gaussian filtering, our goal is pragmatic: to test whether a Bayesian filtering view of selection/attention can retain the efficiency and accuracy of modern deterministic mixers, while yielding interpretable *uncertainty-driven gating* behaviour.

Experimental questions. We address four questions:

Q1 Compute and scaling. How does the parallel implementation of KLA scale with sequence length, and how does it compare to a recurrent (time-stepped) Kalman implementation in wall-clock time?

Q2 Model quality as a single-block primitive. As a drop-in mixer block, do KLA’s update rules match or improve upon deterministic sub-quadratic alternatives (SSMs / linear attention) on controlled synthetic language-modelling tasks that probe core LM skills (long-range dependence, retrieval, and compression)?

Q3 Long-context recall and robustness. Does KLA improve long-context associative recall consistent with uncertainty-weighted filtering?

Q4 State tracking expressivity. Does the fractional-linear structure induced by information-form filtering translate

into stronger state-tracking capabilities (e.g., permutation composition) than linear SSM/attention baselines, while retaining scan-parallelisability?

Finally, we ablate architectural choices within the KLA block to isolate which components contribute to performance and scaling.

5.1. Baselines

We compare KLA against four recent state-of-the-art baselines representing different architectural paradigms for efficient sequence modelling. All baselines use sub-quadratic complexity alternatives to softmax attention. (i) **Recurrent Architectures. mLSTM** (Beck et al., 2024): A modern LSTM variant featuring multiplicative interactions between hidden states and inputs, exponential gating mechanisms, and improved training parallelisation. (ii) **Structured State Space Models. Mamba** (Gu & Dao, 2023): Widely used selective SSM with input-dependent state transition matrices and gating, discussed in Section 3. (iii) **GDN** (Gated Delta Net) (Yang et al., 2024): A delta-rule-based state-space model with selective gating mechanisms for memory updates. Combines principles from associative memory with modern SSM architectures. Represents the current state-of-the-art in SSM-based language modelling. (iv) **Linear Attention. GLA** (Gated Linear Attention) (Yang et al., 2023): A linear attention variant discussed in Section 3, that unifies several modern linear RNN and SSM formulations, including Mamba, under a common framework.

5.2. Compute Scaling of Parallel KLA

Scaling probabilistic / Bayesian primitives to very large context lengths, while retaining efficient end-to-end training parallelism in language modelling, remains a comparatively underexplored area. In practice, achieving competitive scaling and throughput is not only a matter of deriving favourable asymptotic forms (e.g. scan-friendly $\log(T)$ -style structure), but also of realising those gains on modern accelerators via careful kernel-level engineering, as emphasised by recent state-space work (e.g. (Gu & Dao, 2023)).

To make this concrete, we benchmark three KLA implementations that progressively incorporate (i) a naive recurrent (time-stepped) Kalman update, (ii) a mathematically parallel formulation via Torch associative scan, and (iii) a hardware-optimised custom Triton associative-scan kernel. We report forward-only and forward+backward runtimes: the forward-only setting (Figure 11) corresponds to single-batch prompt processing at inference time, while the forward+backward setting (Figure 5) reflects parallel training with batch size 4 (see Section E.2). Overall, the results indicate that information-form filtering admits the same scan-parallel scaling profile as modern SSM/GLA-style mixers, with

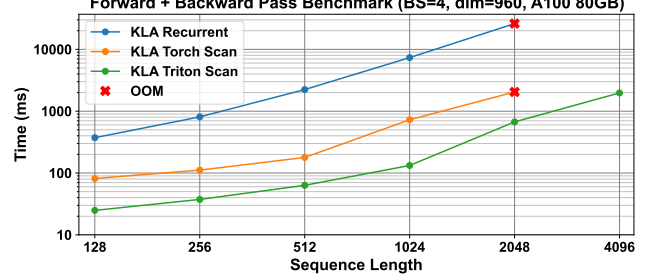


Figure 5. **Training-time runtime scaling.** Wall-clock runtime of KLA implementations across sequence lengths. Torch Scan uses `torch._higher_order_ops.associative_scan`; Triton Scan uses custom forward/backward kernels.

additional speedups unlocked by hardware-level optimisation beyond the pure mathematical reparameterisation. While our Triton kernel already narrows the gap between theory and throughput, additional hardware-level optimisation in the spirit of Mamba/GLA-style fused sequence kernels remains a promising direction.

5.3. KLA as a Language-Modelling Primitive

MAD synthetic LM suite. We evaluate KLA and the baselines as a single block primitive on the MAD-Lab benchmark (Poli et al., 2024), a set of six synthetic token-manipulation tasks that test different LM skills (Table 5). We match parameter counts, effective state sizes, and use a common encoder–decoder training protocol across methods (dataset details in Appendix F; hyperparameters in Appendix G).

Results. Section 5.3 shows that KLA performs competitively across all tasks, matching or surpassing strong deterministic baselines. Gains are most pronounced on tasks that require *selection under corruption* (e.g., *Noisy Recall* and *Selective Copy*), consistent with the interpretation of KLA as performing uncertainty-weighted filtering. In addition, probabilistic decoding (marginalisation under the learned posterior) yields further improvements on noise-corrupted tasks, suggesting that learning posterior variances can provide a useful training signal even without an explicit calibration objective.

Algorithm	Compression	Memorization	Context Recall	Noisy Recall	Fuzzy Recall	Selective Copy
GDN	65.53	99.93	99.94	99.95	37.04	90.30
GLA	49.45	99.99	73.60	85.24	18.22	82.41
Mamba	78.35	99.96	99.92	99.93	30.83	80.60
mLSTM	57.17	99.98	99.98	99.99	25.43	36.61
KLA (Ours)	85.03	98.87	99.95	99.93	45.70	90.67
KLA+ (Ours)	88.87	99.94	99.94	99.95	43.32	91.45

Table 3. Test accuracy (%) on MAD synthetic language-modelling tasks with Gated Delta Network (GDN), Gated Linear Attention (GLA), and KLA with probabilistic decoding (KLA+). Higher values (darker shading) indicate better performance.

Mechanistic behaviour: posterior uncertainty visualisations. To characterise how KLA filters information, we visualise the posterior variance on Selective Copy (Figure 6). Rather than claiming calibrated uncertainty estimation, we use them as a diagnostic of the model’s internal filtering dynamics. In Selective Copy, the posterior variance generally decreases over time as evidence accumulates, while sharp variance spikes align with copy-relevant positions, indicating timesteps where the model treats the input as especially informative for updating its belief.

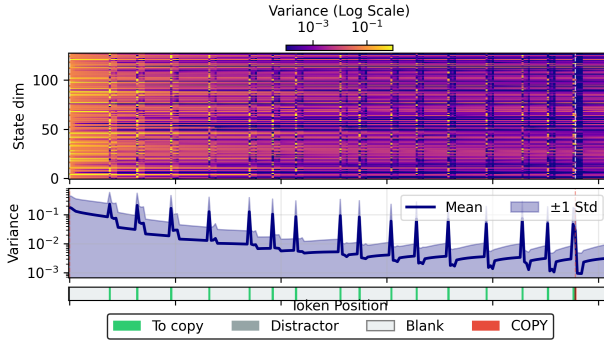


Figure 6. Posterior variance as uncertainty-driven gating. Selective Copy task. **Top:** per-channel variance across state dimensions. **Middle:** average variance over channels. **Bottom:** task structure with green copy tokens. Variance dynamics align with task-relevant tokens, providing an interpretable signal of filtering/selection.

5.4. Long-Context Associative Recall

Multi-Query Associative Recall (MQAR) (Arora et al., 2023) is particularly interesting for fixed-size recurrent architectures, as it directly tests their capacity to store and retrieve multiple key-value associations, a fundamental bottleneck often limited by state dimensionality. MQAR is critical for modern LLMs, where in-context learning relies on retrieving relevant information from extended contexts. Following the Zoology benchmark (Arora et al., 2023), we evaluate KLA on a considerably more difficult configuration than typically studied: sequence length $T = 2048$ with vocabulary size $V = 256$ (matching or exceeding model dimensions; see Table 7 for full configuration). This challenging setting directly probes the *storage capacity* limits of fixed-size recurrent states, requiring many simultaneous associations to be stored and retrieved over long distances.

Figure 7 reveals distinct scaling behaviours across architectures. KLA consistently outperforms Mamba across all dimensions and substantially outperforms GLA, which fails to learn the task under this extreme setting ($T = 2048$, $V = 256$). At lower dimensions ($d = 64$, $d = 128$), GDN performs well; its delta-rule mechanism is specifically designed for strong associative recall at limited capacity (Yang et al., 2024), and it operates with a slightly higher effective state size (see Table 10). At $d = 256$, KLA outperforms all baselines and achieves near-perfect accuracy ($> 95\%$),

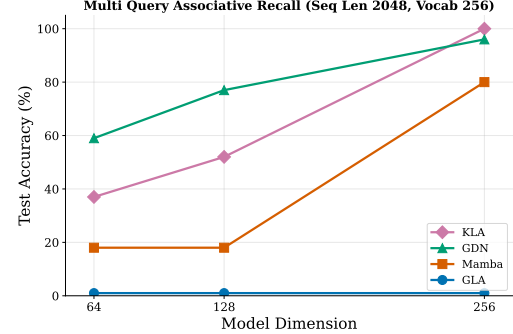


Figure 7. MQAR accuracy vs. model dimension ($T = 2048$, $V = 256$). KLA achieves near-perfect accuracy at dimension 256, outperforming GDN and Mamba. GLA fails to learn the task in this challenging setting.

establishing state-of-the-art performance.

Discussion. We hypothesise that uncertainty-weighted updates help mitigate state “saturation” under heavy key–value load. Unlike purely additive accumulators, KLA’s fractional-linear (Möbius) precision updates (Equation (18)) adaptively down-weight observations based on posterior uncertainty: when the latent state becomes saturated with many associations, high-confidence historical information naturally suppresses unreliable new observations. This provides an implicit, learned compression mechanism, analogous to selective pattern storage in high-capacity associative memories (Storkey & Valabregue, 1997), without requiring explicit dimension scaling.

5.5. State Tracking and Permutation Group Expressivity

Why A_5 matters. A central open question for sub-quadratic sequence models is whether they can *track state* in a way that goes beyond highly-parallel shortcut computation. Recent theory argues that common linear/diagonal SSMs, notably including S4 and Mamba, despite their recurrent form, share expressivity limits similar to transformers in bounded depth: they can be simulated by highly-parallel circuit classes (informally, TC^0), and therefore cannot solve inherently sequential state-tracking problems whose difficulty scales with sequence length. A canonical example is *permutation composition*: computing the product of a sequence of group elements (a word problem). In particular, the word problem for the alternating group A_5 (the smallest non-solvable subgroup of S_5) is used as a minimal, clean benchmark for *hard state tracking*, and it underlies reductions to practical settings such as chess state tracking under certain notations, program evaluation, and entity tracking in narratives (Merrill et al., 2024).

Result. We evaluate KLA on the A_5 permutation composition task following Merrill et al. (2024). Figure 1 shows that KLA solves the task with only 1–2 layers, whereas linear

SSM/attention baselines require increasing depth as sequence length grows in this regime. This behaviour is consistent with KLA’s *fractional-linear* (information-form) updates: while each step remains scan-parallelisable, the resulting state evolution is richer than purely linear recurrences. Taken together, these findings suggest that probabilistic filtering primitives may offer a principled route to improved state tracking without abandoning the parallel scan structure that makes modern SSM/linear-attention models efficient.

5.6. Ablations

Finally, to isolate which components of KLA matter, we perform an ablation with two critical modelling choices. Figure 4 ablates the OU prior discretisation (Section 4.1) on Selective Copy, showing improved stability and accuracy, particularly at greater depth. We report an additional ablation on the importance of the process noise parameter in Appendix E.

6. Conclusion

In this paper, we propose a scalable probabilistic sequence-modelling primitive, the KLA layer, which treats language modelling as a state estimation problem from noisy observations. We show that posterior inference in these models is tractable for very long sequences via parallel scans, and that the resulting gating mechanisms are strictly more expressive than those of modern deterministic linear SSMs and RNNs. Our experiments indicate the promise of KLA as a scalable primitive within the language and probabilistic sequence-modelling toolbox.

7. Limitations and Future Work

We have not explicitly used the posterior covariance for applications where uncertainty quantification may be critical (e.g., epistemic prompt uncertainty, hallucination detection, and OOD prompt detection), which are likely areas where KLA could excel; we leave this for future work. The focus of this work is to evaluate KLA as a *sequence-modelling primitive* and to isolate what the Bayesian filtering update mechanism contributes in a minimal but impactful setting. Accordingly, most experiments use shallow configurations rather than deep, large-scale pretraining. We therefore do not claim state-of-the-art performance on web-scale corpora, very long-context regimes, or open-ended generative benchmarks. Scaling KLA to such settings, as a probabilistic LLM, is left for future work.

Impact Statement

This paper presents work whose goal is to advance the field of Machine Learning. There are many potential societal consequences of our work, none of which we believe must

be specifically highlighted here. The KLA layer provides principled uncertainty quantification, which could benefit applications requiring calibrated predictions, though, as with any language modelling primitive, deployment should consider potential misuse.

Acknowledgements

We thank Henry Gouk, Nikolay Malkin, Thomas Lee, and Stephan Kostov for their valuable feedback on this draft at various stages. We also thank Wouter Boomsma, Frederikke Isa Marin, Jose Cano Reyes, and Jude Harris for the informative discussions over the course of this research. This project has received funding from the European Union’s Horizon Europe research and innovation programme under grant agreement No. 101120726. This work was funded by UK Research and Innovation (UKRI) under the UK government’s Horizon Europe funding Guarantee 10085198.

References

Anderson, B. D. and Moore, J. B. *Optimal filtering*. Courier Corporation, 2005.

Arora, S., Eyuboglu, S., Timalsina, A., Johnson, I., Poli, M., Zou, J., Rudra, A., and Ré, C. Zoology: Measuring and improving recall in efficient language models. *arXiv preprint arXiv:2312.04927*, 2023.

Beck, M., Pöppel, K., Spanring, M., Auer, A., Prudnikova, O., Kopp, M., Klambauer, G., Brandstetter, J., and Hochreiter, S. xlSTM: Extended long short-term memory. *Advances in Neural Information Processing Systems*, 37: 107547–107603, 2024.

Becker, P., Pandya, H., Gebhardt, G., Zhao, C., Taylor, C. J., and Neumann, G. Recurrent Kalman networks: Factorized inference in high-dimensional deep feature spaces. In *Proceedings of the 36th International Conference on Machine Learning*, volume 97 of *Proceedings of Machine Learning Research*, pp. 544–552. PMLR, 2019.

Becker, P., Freymuth, N., and Neumann, G. KalMamba: Towards efficient probabilistic state space models for RL under uncertainty. In *ICML 2024 Workshop: Aligning Reinforcement Learning Experimentalists and Theorists*, 2024.

Blelloch, G. E. Prefix sums and their applications. In *Synthesis of Parallel Algorithms*, pp. 35–60. Morgan Kaufmann, 1990.

Broadbent, D. E. A mechanical model for human attention and immediate memory. *Psychological review*, 64(3):205, 1957.

Dao, T. and Gu, A. Transformers are ssms: Generalized models and efficient algorithms through structured state space duality. *arXiv preprint arXiv:2405.21060*, 2024.

Deutsch, J. A. and Deutsch, D. Attention: Some theoretical considerations. *Psychological review*, 70(1):80, 1963.

Feldman, H. and Friston, K. J. Attention, uncertainty, and free-energy. *Frontiers in human neuroscience*, 4:215, 2010.

Fraccaro, M., Sønderby, S. K., Paquet, U., and Winther, O. Sequential neural models with stochastic layers. In *Advances in Neural Information Processing Systems*, volume 29, pp. 2207–2215, 2016.

Gu, A. and Dao, T. Mamba: Linear-time sequence modeling with selective state spaces. *arXiv preprint arXiv:2312.00752*, 2023.

Gu, A., Goel, K., and Re, C. Efficiently modeling long sequences with structured state spaces. In *International Conference on Learning Representations*, 2021.

Gupta, A., Gu, A., and Berant, J. Diagonal state spaces are as effective as structured state spaces. In *Advances in Neural Information Processing Systems*, volume 35, pp. 22982–22994, 2022.

Haarnoja, T., Tang, H., Abbeel, P., and Levine, S. Reinforcement learning with deep energy-based policies. In *International Conference on Machine Learning*, volume 70 of *Proceedings of Machine Learning Research*, pp. 1352–1361. PMLR, 2017.

Hafner, D., Lillicrap, T., Fischer, I., Villegas, R., Ha, D., Lee, H., and Davidson, J. Learning latent dynamics for planning from pixels. In *Proceedings of the 36th International Conference on Machine Learning*, volume 97 of *Proceedings of Machine Learning Research*, pp. 2555–2565. PMLR, 2019.

Hafner, D., Lillicrap, T., Ba, J., and Norouzi, M. Dream to control: Learning behaviors by latent imagination. In *International Conference on Learning Representations*, 2020.

Kalman, R. E. A new approach to linear filtering and prediction problems. *Transactions of the ASME-Journal of Basic Engineering*, 82(Series D):35–45, 1960.

Karl, M., Sölch, M., Bayer, J., and van der Smagt, P. Deep variational Bayes filters: Unsupervised learning of state space models from raw data. In *Proceedings of the International Conference on Learning Representations*, 2017.

Katharopoulos, A., Vyas, A., Pappas, N., and Fleuret, F. Transformers are RNNs: Fast autoregressive transformers with linear attention. In *International conference on machine learning*, pp. 5156–5165. PMLR, 2020.

Khan, M. E. Matrix inversion lemma and information filter. *Honeywell Techonology Solutions Lab, Bangalore, India*, 2005.

Kingma, D. P. and Ba, J. Adam: A method for stochastic optimization. In *International Conference on Learning Representations*, 2015.

Krishnan, R. G., Shalit, U., and Sontag, D. Deep Kalman filters. *arXiv preprint arXiv:1511.05121*, 2015.

Krishnan, R. G., Shalit, U., and Sontag, D. Structured inference networks for nonlinear state space models. In *Proceedings of the Thirty-First AAAI Conference on Artificial Intelligence*, pp. 2101–2109, 2017.

Luis, C. E., Bottero, A. G., Vinogradsk, J., Berkenkamp, F., and Peters, J. Uncertainty representations in state-space layers for deep reinforcement learning under partial observability. *arXiv preprint arXiv:2409.16824*, 2024.

Merrill, W., Petty, J., and Sabharwal, A. The illusion of state in state-space models. *arXiv preprint arXiv:2404.08819*, 2024.

Muca Cirone, N., Orvieto, A., Walker, B., Salvi, C., and Lyons, T. Theoretical foundations of deep selective state-space models. *Advances in Neural Information Processing Systems*, 37:127226–127272, 2024.

Nielsen, F. and Garcia, V. Statistical exponential families: A digest with flash cards. *arXiv preprint arXiv:0911.4863*, 2009.

Paszke, A., Gross, S., Massa, F., Lerer, A., Bradbury, J., Chanan, G., Killeen, T., Lin, Z., Gimelshein, N., Antiga, L., Desmaison, A., Kopf, A., Yang, E., DeVito, Z., Raison, M., Tejani, A., Chilamkurthy, S., Steiner, B., Fang, L., Bai, J., and Chintala, S. PyTorch: An Imperative Style, High-Performance Deep Learning Library. In *Advances in Neural Information Processing Systems*, volume 32. Curran Associates, Inc., 2019.

Poli, M., Thomas, A. W., Nguyen, E., Ponnusamy, P., Deiseroth, B., Kersting, K., Suzuki, T., Hie, B., Ermon, S., Re, C., Zhang, C., and Massaroli, S. Mechanistic design and scaling of hybrid architectures. In *Proceedings of the 41st International Conference on Machine Learning*, volume 235 of *Proceedings of Machine Learning Research*, pp. 40908–40950. PMLR, 2024.

Rao, R. P. and Ballard, D. H. Predictive coding in the visual cortex: a functional interpretation of some extra-classical receptive-field effects. *Nature neuroscience*, 2(1):79–87, 1999.

Särkkä, S. and García-Fernández, Á. F. Temporal parallelization of bayesian smoothers. *IEEE Transactions on Automatic Control*, 66(1):299–306, 2020.

Shaj, V., Becker, P., Büchler, D., Pandya, H., van Duijkeren, N., Taylor, C. J., Hanheide, M., and Neumann, G. Action-conditional recurrent kalman networks for forward and inverse dynamics learning. In *Conference on Robot Learning*, pp. 765–781. PMLR, 2021.

Shaj Kumar, V., Gholam Zadeh, S., Demir, O., Douat, L., and Neumann, G. Multi time scale world models. *Advances in Neural Information Processing Systems*, 36:26764–26775, 2023.

Smith, J. T., Warrington, A., and Linderman, S. Simplified state space layers for sequence modeling. In *The Eleventh International Conference on Learning Representations*, 2022.

Storkey, A. and Valabregue, R. Hopfield learning rule with high capacity storage of time-correlated patterns. *Electronics Letters*, 33:1803 – 1804, 11 1997.

Tillet, P., Kung, H.-T., and Cox, D. Triton: an intermediate language and compiler for tiled neural network computations. In *Proceedings of the 3rd ACM SIGPLAN International Workshop on Machine Learning and Programming Languages*, pp. 10–19, 2019.

Treisman, A. M. Strategies and models of selective attention. *Psychological review*, 76(3):282, 1969.

Vaswani, A., Shazeer, N., Parmar, N., Uszkoreit, J., Jones, L., Gomez, A. N., Kaiser, Ł., and Polosukhin, I. Attention is all you need. *Advances in neural information processing systems*, 30, 2017.

Watter, M., Springenberg, J. T., Boedecker, J., and Riedmiller, M. A. Embed to control: A locally linear latent dynamics model for control from raw images. In *Advances in Neural Information Processing Systems*, volume 28, pp. 2746–2754, 2015.

Yang, S., Wang, B., Shen, Y., Panda, R., and Kim, Y. Gated linear attention transformers with hardware-efficient training. *arXiv preprint arXiv:2312.06635*, 2023.

Yang, S., Kautz, J., and Hatamizadeh, A. Gated delta networks: Improving Mamba2 with delta rule. *arXiv preprint arXiv:2412.06464*, 2024.

Yu, A. and Erichson, N. B. Block-biased mamba for long-range sequence processing. *arXiv preprint arXiv:2505.09022*, 2025.

Appendix

Appendix outline

- Appendix A: Architecture Details (p. 14)
 - Figure 5: Model Architecture Diagram (p. 14)
 - Algorithm 1: Kalman Linear Attention (p. 15)
 - Training Loss
- Appendix B: Notation (p. 16)
- Appendix C: Extended Background (p. 16)
 - Möbius / Fractional-Linear Transformations (p. 16)
 - Information Form of Gaussian Distributions (p. 16)
 - Kalman and Information Filters (p. 17)
- Appendix D: Theorems and Proofs (p. 19)
- Appendix E: Additional Empirical Results (p. 22)
 - Ablation On The Importance Of Process Noise Parameter (p. 22)
 - Forward Pass Runtime Scaling (p. 22)
 - Equivalent Attention Matrix (p. 22)
 - Attention Map Visualisation (p. 23)
- Appendix F: Datasets and Benchmarks Used (p. 26)
 - MAD LM Suite (p. 26)
 - Long-Context MQAR (p. 27)
- Appendix G: Hyperparameters Used (p. 28)
 - Experimental Protocol (p. 28)
 - Training Hyperparameters (p. 28)
 - MAD-Lab Hyperparameters (p. 28)
 - MQAR Hyperparameters (p. 28)
 - A5 State Tracking Hyperparameters (p. 29)

A. Architecture Details

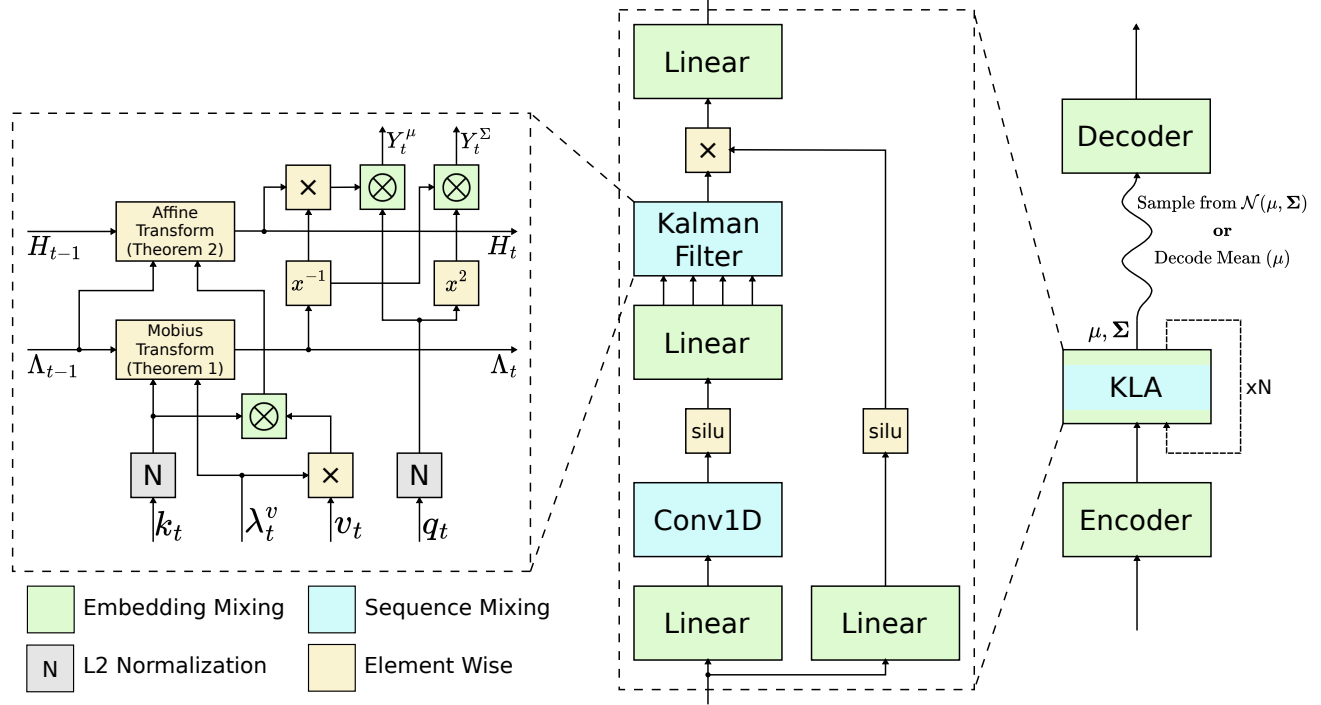


Figure 8. Model architecture used in our experiments. The KLA block is a drop-in replacement for Transformer or SSM blocks. We follow a similar block structure to Mamba, fusing the sequence mixing and gated MLP into a single block. We additionally employ QK-Norm and use an expansion factor of 1. Tokens are embedded and passed through a *sequence mixer*, then decoded to logits. The sequence mixer is a drop-in primitive that can be instantiated as attention variants, or other SSM/Filter modules. Many mixers are paired with standard *scaffolding*—e.g., 1D convolutions, residual/skip connections, and simple nonlinearities (elementwise multiplication or activations)—shown on the right.

Architecture. We use a consistent language modelling architecture across all models and baselines, as illustrated in Figure 8. The architecture follows a standard pattern: input tokens are embedded, passed through a sequence mixer layer, and then decoded to output logits. The sequence mixer serves as a drop-in primitive that can be instantiated as KLA, Mamba, GLA, or other SSM/attention variants.

Following the Mamba design, we employ standard scaffolding components paired with the sequence mixer: a 1D causal convolution with kernel size 4 and SiLU activation, along with residual connections and simple nonlinearities (elementwise multiplication). We use standard state expansion (see Section 3) and is set to 16 (N or sometimes called d_{state} in SSM codebases) as default similar to (Gu & Dao, 2023). More extensive exploration of scaffolding configurations optimally suited to the KLA filtering mixer can be a direction for future work.

We implemented KLA with PyTorch (Paszke et al., 2019) and used the Adam optimiser (Kingma & Ba, 2015) for training the models.

Training loss. We consider two training losses. Throughout, the decoder is applied to the query-conditioned readout $\mathbf{y}_t = \mathbf{q}_t \odot \mathbf{z}_t$; when the readout noise is zero this is a deterministic linear map, so conditioning on \mathbf{z}_t or \mathbf{y}_t is equivalent up to this transformation.

(i) Posterior mean: logits $\ell_t = g_\theta(\mathbf{y}_t)$ are obtained from the posterior-mean readout $\mathbf{y}_t = \mathbf{q}_t \odot \mu_t$ and trained with cross-entropy.

(ii) Log marginal likelihood: minimises the negative log marginal likelihood of the output token o_t under the latent

Algorithm 1 Kalman Linear Attention

```

1: Input:  $\mathbf{X} : (B, T, 1, D)$ 
2: Output  $\mathbf{Y}^\mu : (B, T, 1, D)$ 
3: Output (Optional)  $\mathbf{Y}^\Sigma : (B, T, 1, D)$ 
4:  $\mathbf{A}, \mathbf{P}, \Delta : (N, D) \leftarrow \text{Parameters}$   $\triangleright A: \text{Gating/decay}, P: \text{Process noise}, \Delta: \text{Discretisation step size}$ 
5:  $\mathbf{K} : (B, T, N, 1) \leftarrow f_{\theta_k}(\mathbf{X})$   $\triangleright \mathbf{K}: \text{Observation operator}$ 
6:  $\mathbf{Q} : (B, T, 1, N) \leftarrow f_{\theta_q}(\mathbf{X})$   $\triangleright \mathbf{Q}: \text{Readout operator}$ 
7:  $\mathbf{V}, \mathbf{\Lambda}^v : (B, T, 1, D) \leftarrow f_{\theta_{v, \lambda^v}}(\mathbf{X})$   $\triangleright \mathbf{V}: \text{Observation mean and precision}, \lambda^v \in \mathbb{R}^+$ 
8:  $\bar{\mathbf{A}} : (N, D) \leftarrow \text{OU-Discretisation}(\mathbf{A}, \Delta)$   $\triangleright \text{See Equation (8)}$ 
9:  $\bar{\mathbf{P}} : (N, D) \leftarrow \text{OU-Discretisation}(\mathbf{A}, \mathbf{P}, \Delta)$ 
10:  $\mathbf{\Lambda} : (B, T, N, D) \leftarrow \text{Mobius-Scan}(\mathbf{K}, \mathbf{\Lambda}^v, \bar{\mathbf{P}}, \bar{\mathbf{A}})$   $\triangleright \text{See Equation (16)}$ 
11:  $\mathbf{H} : (B, T, N, D) \leftarrow \text{Linear-Scan}(\mathbf{K}, \mathbf{\Lambda}^v, \mathbf{V}, \mathbf{\Lambda}, \bar{\mathbf{P}}, \bar{\mathbf{A}})$   $\triangleright \text{See Equation (19)}$ 
12:  $\mathbf{Y}^\mu : (B, T, 1, D) \leftarrow \mathbf{Q}(\mathbf{H}\mathbf{\Lambda}^{-1})$ 
13: if Decode Variance then
14:    $\mathbf{Y}^\Sigma : (B, T, 1, D) \leftarrow \mathbf{Q}^2 \mathbf{\Lambda}^{-1}$ 
15:   Return:  $\mathbf{Y}^\mu, \mathbf{Y}^\Sigma$ 
16: else
17:   Return:  $\mathbf{Y}^\mu$ 
18: end if

```

posterior,

$$\begin{aligned}
 -\log p_\theta(o_t \mid \mathbf{X}) &= -\log \int \underbrace{p_\theta(o_t \mid \mathbf{y}_t)}_{\text{decoder}} \underbrace{p_\theta(\mathbf{z}_t \mid \mathbf{X})}_{\text{KLA posterior}} d\mathbf{z}_t \\
 &\approx -\log \left(\frac{1}{S} \sum_{s=1}^S p_\theta(o_t \mid \mathbf{y}_t^{(s)}) \right), \tag{21}
 \end{aligned}$$

with $\mathbf{z}_t^{(s)} \sim p_\theta(\mathbf{z}_t \mid \mathbf{X})$ and $\mathbf{y}_t^{(s)} = \mathbf{q}_t \odot \mathbf{z}_t^{(s)}$. Equivalently, the estimator can be written as a logsumexp:

$$\begin{aligned}
 -\log p_\theta(o_t \mid \mathbf{X}) &\approx -\log \left(\frac{1}{S} \sum_{s=1}^S p_\theta(o_t \mid \mathbf{y}_t^{(s)}) \right) \\
 &= -\text{logsumexp} \left(\log p_\theta(o_t \mid \mathbf{y}_t^{(s)}) \right) + \log S, \tag{22}
 \end{aligned}$$

which reduces to cross-entropy when $S=1$. We show this for a single time-step; it can be trivially extended across timesteps.

B. Notation

Throughout the paper we use the following convention:

Symbol	Meaning
t	Time index
z_t	Latent state at time t
v_t	Value (observed token/features) at time t
A_t	State transition matrix
P_t	Process noise covariance (discretized: \bar{P}_t)
C_t	Observation (likelihood) matrix
Λ_t^v	Value precision (inverse observation variance)
$\mathcal{N}(\mu, \Sigma)$	Gaussian in <i>moment</i> form
$\mathcal{N}(\eta, \Lambda)$	Gaussian in <i>canonical</i> form; $\eta = \Lambda\mu$, $\Lambda = \Sigma^{-1}$
$\mu_t^{\text{prior}}, \Sigma_t^{\text{prior}}$	Predictive prior mean/cov at t (canonical: $\eta_t^{\text{prior}}, \Lambda_t^{\text{prior}}$)
μ_t, Σ_t	Posterior mean/cov at t (canonical: η_t, Λ_t)
Beliefs (linear–Gaussian case):	
$z_t v_{1:t-1} \sim \mathcal{N}(\mu_t^{\text{prior}}, \Sigma_t^{\text{prior}})$	(predictive prior)
$z_t v_{1:t} \sim \mathcal{N}(\mu_t, \Sigma_t)$	(posterior)

Diagonal (per-dimension) specialisation. When matrices are diagonal, we identify them with their diagonal vectors and switch to bold lowercase: $A_t \equiv \mathbf{a}_t$, $B_t \equiv \mathbf{b}_t$, $K_t \equiv \mathbf{k}_t$ (key), $P_t \equiv \mathbf{p}_t$ (process noise); value precision Λ_t^v is treated as a scalar. All algebra becomes *elementwise*: products use the Hadamard operator \odot , superscripts like \mathbf{a}_t^2 denote elementwise squares, and $(\cdot)^{-1}$ on lowercase vectors means elementwise inverse.

Full (matrix)	Diagonal notation (this paper)	Implication (elementwise)
A_t	\mathbf{a}_t	$(A_t \mathbf{x}) = \mathbf{a}_t \odot \mathbf{x}$; $A_t^2 \Rightarrow \mathbf{a}_t^2$
K_t	\mathbf{k}_t	$K_t \Sigma K_t^\top \Rightarrow \mathbf{k}_t^2 \odot \Sigma$ (key)
P_t	\mathbf{p}_t	Process noise cov.; $\bar{P}_t \Rightarrow \bar{\mathbf{p}}_t$ (discretized)
Λ_t^v	Λ_t^v	Scalar value precision (variance = $(\Lambda_t^v)^{-1}$)

C. Extended Background

C.1. Möbius / Fractional-Linear Transformations.

A Möbius (a.k.a. fractional-linear) transformation is the map

$$z \mapsto \frac{az + b}{cz + d}, \quad ad - bc \neq 0.$$

It generalises the familiar affine form ($c = 0$ gives $az + b$) by introducing an additional denominator term. Each transform is represented (up to multiplication by a nonzero scalar) by a 2×2 matrix $M = \begin{pmatrix} a & b \\ c & d \end{pmatrix}$ and acts on a scalar z via the linear-fractional rule

$$M(z) := \frac{az + b}{cz + d}.$$

Composing multiple transforms amounts to multiplying their representing matrices, so associativity and invertibility (whenever $\det M \neq 0$) follow directly. Geometrically, Möbius transforms can be viewed as compositions of translations, rotations/scalings, and a crucial nonlinear ingredient—*inversion*—which affine transformations cannot capture. The denominator also provides a built-in *self-normalisation*: as the state grows, it is automatically rescaled, producing saturation and stability effects reminiscent of gating or normalisation layers, but achieved directly through the update itself.

C.2. Information Form of Gaussian Distributions and Information Filters.

Gaussians belong to the exponential family (Nielsen & Garcia, 2009), so the posterior can be written in *canonical* (information) form with precision $\Lambda_t = \Sigma_t^{-1}$ and natural parameter $\eta_t = \Lambda_t \mu_t$. Filtering recursions in this parameterisation

are known as *information filters (IF)* (Anderson & Moore, 2005; Khan, 2005). They are algebraically equivalent to the standard (moment) Kalman updates; only the representation of the Gaussian belief differs. Crucially, the canonical posterior updates are *linear-additive* in (η_t, Λ_t) , a property we leverage for scalable sequence modelling in Section 4.

C.3. Control vs Observation View Of Token Processing

State-space models can be understood from two complementary perspectives (Figure 9):

Observation view (traditional SSM/Kalman filter). In classical Bayesian filtering, input tokens are treated as *noisy observations* of a hidden state. The model assumes: (i) a latent state z_t evolves over time via learned dynamics, and (ii) each token v_t is a noisy measurement generated from this state. The goal is to *infer* the hidden state from the observed tokens—asking “what underlying state could have produced these observations?”

Control view (Mamba/S6). In contrast, Mamba treats input tokens as *control signals* that directly drive the state. There is no observation noise or inference step; tokens deterministically update the hidden state via $z_t = \bar{A}_t z_{t-1} + \bar{B}_t u_t$. The state simply accumulates information from inputs—asking “how should I update my memory given this new input?”

Why this matters. The observation view naturally provides uncertainty quantification: since tokens are noisy measurements, the model maintains a posterior *distribution* over states rather than a point estimate. This is the foundation of KLA—we treat language modelling as Bayesian filtering where tokens inform our belief about an underlying semantic state.

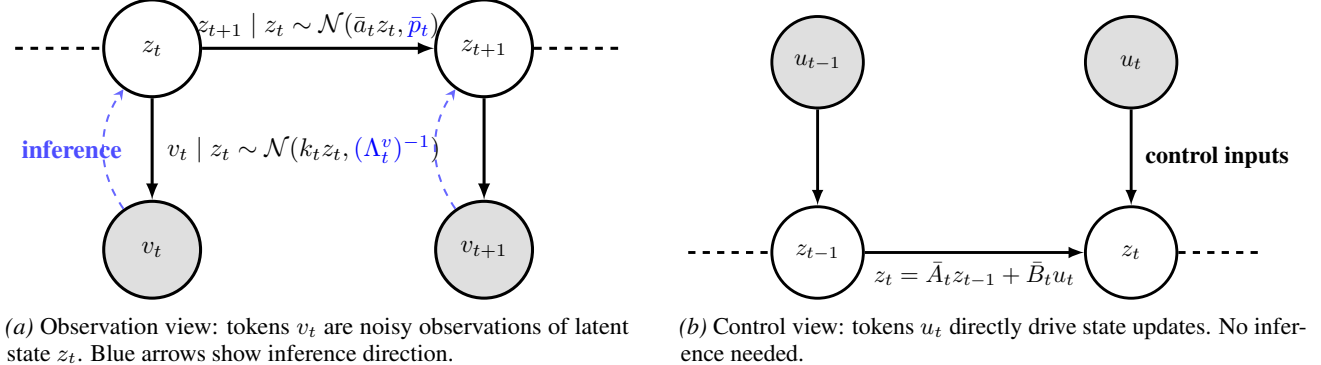


Figure 9. Two views of state-space sequence models. **Left:** Bayesian/observation view—tokens are measurements, inference recovers hidden state. **Right:** Control view (Mamba)—tokens are inputs that deterministically update state.

C.4. Kalman and Information Filters

C.4.1. BAYESIAN FILTERING AS POSTERIOR INFERENCE.

Bayesian filters (Kalman, information-filter variants) are *inference schemes*—procedures that compute posterior beliefs about latent states from noisy data. The Kalman filter assumes a Gaussian linear state-space model: the latent evolves via a (possibly time-varying) linear transition A_t with unmodelled variability captured by process noise Q_t , and each observed token feature o_t is generated by an observation model C_t with observation noise covariance Σ_t^{obs} . The filter then computes $p(z_t | o_{1:t})$ sequentially by combining the dynamics prior with token evidence.

In this linear–Gaussian setting, inference has closed-form solutions: in the *moment parametrisation* (μ_t, Σ_t) the scheme is called the **Kalman filter**, while in the *canonical parametrisation* (η_t, Λ_t) it is called the **information filter**. Both are algebraically equivalent, differing only in how Gaussian beliefs are represented.

Intuition on noise. In our linear–Gaussian state-space model, the “noise” terms w_t and v_t are not claims that language or the world is intrinsically random; they compactly represent *uncertainty* and unmodelled effects (domain shift, annotation/embedding error, missing context). Their covariances P_t and Σ_t^{obs} calibrate trust in dynamics vs. data—larger P_t yields more adaptivity (faster forgetting), while larger Σ_t^{obs} leans on the prior—producing principled “gates” via precision ratios. In contrast, ‘noise’ in diffusion models is an *algorithmic corruption* deliberately added in a forward process to define a denoising/score-matching objective; its schedule (β_t) is chosen for optimisation/SNR shaping rather than for model

Belief / Parameters	Kalman Filter (moment form)	Information Filter (canonical form)
Prior / Prediction $z_t v_{1:t-1} \sim \mathcal{N}(\mu_t^{\text{prior}}, \Sigma_t^{\text{prior}})$	$\mu_t^{\text{prior}} = A_t \mu_{t-1}$ $\Sigma_t^{\text{prior}} = A_t \Sigma_{t-1} A_t^\top + P_t$	$\eta_t^{\text{prior}} = \Lambda_t^{\text{prior}} A_t \Lambda_{t-1}^{-1} \eta_{t-1}$ $\Lambda_t^{\text{prior}} = (A_t \Lambda_{t-1}^{-1} A_t^\top + P_t)^{-1}$
Posterior / Update $z_t v_{1:t} \sim \mathcal{N}(\mu_t, \Sigma_t)$	$\mu_t = \mu_t^{\text{prior}} + K_t (v_t - C_t \mu_t^{\text{prior}})$ $\Sigma_t = (I - K_t C_t) \Sigma_t^{\text{prior}}$ $K_t = \Sigma_t^{\text{prior}} C_t^\top (C_t \Sigma_t^{\text{prior}} C_t^\top + (\Lambda_t^{\text{v}})^{-1})^{-1}$	$\Lambda_t = \Lambda_t^{\text{prior}} + C_t^\top \Lambda_t^{\text{v}} C_t$ $\eta_t = \eta_t^{\text{prior}} + C_t^\top \Lambda_t^{\text{v}} v_t$

Table 4. Two equivalent views at time t : moment (KF) vs. canonical (IF). Superscript “prior” denotes the predictive prior; unadorned symbols denote the posterior.

measurement uncertainty.

D. Theorems and Proofs

Theorem 1 (Precision Update as a Möbius Transformation). *Let λ_t be the posterior precision at time t in the diagonal linear–Gaussian model Equation (7)–Equation (9). Define $\phi_t := \mathbf{k}_t^2 \odot \Lambda_t^v$. Then the map $\lambda_{t-1} \mapsto \lambda_t$ is a linear-fractional (Möbius) transform:*

$$\lambda_t = \mathbf{M}_t(\lambda_{t-1}) = \frac{\alpha_t \odot \lambda_{t-1} + \beta_t}{\gamma_t \odot \lambda_{t-1} + \delta_t}, \quad (16)$$

$$\mathbf{M}_t = \begin{pmatrix} \alpha_t & \beta_t \\ \gamma_t & \delta_t \end{pmatrix} = \begin{pmatrix} 1 + \bar{\mathbf{p}}_t \odot \phi_t & \bar{\mathbf{a}}_t^2 \odot \phi_t \\ \bar{\mathbf{p}}_t & \bar{\mathbf{a}}_t^2 \end{pmatrix}. \quad (17)$$

Proof of Theorem 1. Consider the 1D (or diagonal) linear–Gaussian state space model

$$z_t = a_t z_{t-1} + \varepsilon_t, \quad \varepsilon_t \sim \mathcal{N}(0, p_t), \quad v_t = k_t z_t + \nu_t, \quad \nu_t \sim \mathcal{N}(0, (\Lambda_t^v)^{-1}),$$

and define the posterior precision $\lambda_t := \text{Var}(z_t \mid v_{1:t})^{-1}$.

Step 1 (Information-form predict/update).

$$(\text{predict}) \quad \lambda_t^{\text{prior}} = (a_t^2 \lambda_{t-1}^{-1} + p_t)^{-1} = \frac{\lambda_{t-1}}{a_t^2 + p_t \lambda_{t-1}}, \quad (\text{update}) \quad \lambda_t = \lambda_t^{\text{prior}} + k_t^2 \Lambda_t^v.$$

Step 2 (Single-step recursion and rearrangement). Eliminate the intermediate λ_t^{prior} to obtain

$$\lambda_t = \frac{\lambda_{t-1}}{a_t^2 + p_t \lambda_{t-1}} + k_t^2 \Lambda_t^v = \frac{(1 + p_t k_t^2 \Lambda_t^v) \lambda_{t-1} + a_t^2 k_t^2 \Lambda_t^v}{p_t \lambda_{t-1} + a_t^2}.$$

Hence λ_t is a linear–fractional (Möbius) transform of λ_{t-1} ,

$$\lambda_t = M_t(\lambda_{t-1}) = \frac{\alpha_t \lambda_{t-1} + \beta_t}{\gamma_t \lambda_{t-1} + \delta_t}, \quad M_t = \begin{pmatrix} \alpha_t & \beta_t \\ \gamma_t & \delta_t \end{pmatrix} = \begin{pmatrix} 1 + p_t \phi_t & a_t^2 \phi_t \\ p_t & a_t^2 \end{pmatrix},$$

where $\phi_t := k_t^2 \Lambda_t^v$. Thus, the precision recursion is a Möbius transformation with the stated matrix form. The diagonal multivariate case follows by applying the same scalar derivation to each diagonal element. □

Corollary 1 (Precision Updates via Parallel Prefix Scan). *Given λ_0 and matrices $\{\mathbf{M}_t\}_{t=1}^T$ from Theorem 1, the posterior precisions $\{\lambda_t\}_{t=1}^T$ can be computed by a parallel prefix scan over $\{\mathbf{M}_t\}$ with $\mathcal{O}(T)$ work and $\mathcal{O}(\log T)$ depth.*

Proof of Corollary 1. By Theorem 1, each precision update is a Möbius transformation: $\lambda_t = M_t(\lambda_{t-1})$. Since Möbius transformations compose via matrix multiplication, the precision at time t can be expressed as

$$\lambda_t = M_t \circ M_{t-1} \circ \dots \circ M_1(\lambda_0) = (M_t \cdot M_{t-1} \cdots M_1) \cdot \lambda_0,$$

where the composition $M_{1:t} := \prod_{s=1}^t M_s$ is computed via standard 2×2 matrix multiplication. Since matrix multiplication is associative, the product $M_{1:T}$ can be computed via a parallel prefix scan (Blelloch, 1990) with $\mathcal{O}(T)$ work and $\mathcal{O}(\log T)$ depth on T processors. Once the prefix products $\{M_{1:t}\}_{t=1}^T$ are available, each precision $\lambda_t = M_{1:t} \cdot \lambda_0$ is obtained in $\mathcal{O}(1)$ time, yielding the claimed complexity. □

Remark (Practical Implementation). *In practice, the parallel prefix scan can be implemented efficiently on modern hardware using frameworks such as JAX’s `lax.associative_scan` or PyTorch’s parallel primitives. The $\mathcal{O}(\log T)$ depth translates to logarithmic wall-clock time on sufficiently parallel hardware, matching the computational efficiency of deterministic SSMs like Mamba while maintaining probabilistic semantics.*

Theorem 2 (Mean Update as Affine Transformations). *Let $\eta_t := \lambda_t \odot \mu_t$ be the posterior information mean and Λ_t^v the value precision. Given the precision path $\{\lambda_t\}$, the information mean evolves affinely:*

$$\eta_t = \underbrace{(\bar{\mathbf{a}}_t^2 + \bar{\mathbf{p}}_t \odot \lambda_{t-1})^{-1} \odot \bar{\mathbf{a}}_t \odot \eta_{t-1}}_{f_t \text{ (history-dependent forget gate)}} + \underbrace{\mathbf{k}_t \odot \Lambda_t^v \odot \mathbf{v}_t}_{\text{token evidence}}. \quad (19)$$

Proof of Theorem 2. Write the information parameters as $\eta_t := \Lambda_t \mu_t$ and let Λ_t^v denote the value precision. The information-form measurement update is

$$\Lambda_t = \Lambda_t^{\text{prior}} + k^2 \Lambda_t^v, \quad \eta_t = \eta_t^{\text{prior}} + k \Lambda_t^v v_t,$$

so the observation contribution is affine with coefficient $k \Lambda_t^v$.

For the time-prediction of the information mean, use $\mu_t^{\text{prior}} = a \mu_{t-1}$ and $\eta_t^{\text{prior}} = \Lambda_t^{\text{prior}} \mu_t^{\text{prior}}$. Eliminating the means gives

$$\eta_t^{\text{prior}} = \Lambda_t^{\text{prior}} a \mu_{t-1} = \Lambda_t^{\text{prior}} a \Lambda_{t-1}^{-1} \eta_{t-1}.$$

Hence, given the (known) precision path $\{\Lambda_t, \Lambda_t^{\text{prior}}\}$,

$$\eta_t = \underbrace{(\Lambda_t^{\text{prior}} a \Lambda_{t-1}^{-1})}_{f_t} \eta_{t-1} + k \Lambda_t^v v_t, \quad \mu_t = \Lambda_t^{-1} \eta_t.$$

This proves the claimed affine form. \square

Theorem 3 (Convolutional Form for Deterministic LTI Systems). *Under the conditions: (i) time-invariant dynamics, $\mathbf{a}_t \equiv \mathbf{a}$, $\mathbf{k}_t \equiv \mathbf{k}$; and (ii) deterministic dynamics, process noise $\mathbf{p}_t = \mathbf{0}$, both the precision and information mean updates reduce to block-Toeplitz convolutions computable in $\mathcal{O}(T \log T)$ time via FFT/NTT:*

Precision updates: $\Lambda_t = \sum_{s=0}^t \mathbf{a}^{-2(t-s)} \odot \mathbf{k}^2 \odot \Lambda_s^v$

Information mean updates: $\eta_t = \mathbf{k} \odot \sum_{s=0}^t \mathbf{a}^{t-s} \odot \Lambda_s^v \odot \mathbf{v}_s, \quad \mu_t = \Lambda_t^{-1} \odot \eta_t$

Proof of Theorem 3. When $p_t = 0$ (deterministic dynamics), the Möbius transformation from Theorem 1 simplifies. Specifically, with zero process noise, the precision recursion becomes $\lambda_t = a^{-2} \lambda_{t-1} + k^2 \Lambda_t^v$. For time-invariant a and k , this unrolls to:

$$\lambda_t = a^{-2t} \lambda_0 + k^2 \sum_{s=0}^t a^{-2(t-s)} \Lambda_s^v$$

which is a discrete convolution with kernel $\kappa[n] = k^2 a^{-2n}$.

Similarly, from Theorem 2, when $p_t = 0$ we have $f_t = a^{-1}$ constant, so the information mean recursion $\eta_t = a^{-1} \eta_{t-1} + k \Lambda_t^v v_t$ unrolls to:

$$\eta_t = k \sum_{s=0}^t a^{t-s} \Lambda_s^v v_s$$

which is also a convolution with kernel $h[n] = k a^n$.

Both convolutions have Toeplitz structure and can be computed via FFT in $\mathcal{O}(\log T)$ parallel time using the convolution theorem. \square

Remark (Practical Note). *While theoretically interesting, the convolutional form is primarily relevant for perfectly deterministic systems ($\mathbf{p} = \mathbf{0}$). In practice, KLA uses the more general parallel scan formulation (Corollary 1) which handles stochastic dynamics ($\mathbf{p}_t > \mathbf{0}$) efficiently.*

Corollary 2 (Mean Updates via Parallel Prefix Scan). *The posterior information means $\{\eta_t\}_{t=1}^T$ are computable via parallel prefix scan over the affine transformations in Theorem 2 in $\mathcal{O}(T)$ work and $\mathcal{O}(\log T)$ depth.*

Proof of Corollary 2. From Theorem 2, the information mean update has the affine form:

$$\eta_t = f_t \eta_{t-1} + k_t \Lambda_t^V v_t$$

where $f_t = \frac{a_t}{a_t^2 + p_t \lambda_{t-1}}$ (which simplifies to a^{-1} when $p_t = 0$).

Define the binary associative operator \oplus on pairs (f, b) by:

$$(f_2, b_2) \oplus (f_1, b_1) = (f_2 f_1, f_2 b_1 + b_2)$$

This is the standard associative operator for affine transformations.

The composed transformation at time t is:

$$(f_{1:t}, b_{1:t}) = (f_t, k_t \Lambda_t^V v_t) \oplus (f_{t-1}, k_{t-1} \Lambda_{t-1}^V v_{t-1}) \oplus \cdots \oplus (f_1, k_1 \Lambda_1^V v_1)$$

which gives $\eta_t = f_{1:t} \eta_0 + b_{1:t}$.

Since \oplus is associative, the sequence of compositions can be computed via a parallel prefix scan (Blelloch, 1990) with $\mathcal{O}(T)$ work and $\mathcal{O}(\log T)$ depth. Once all information means $\{\eta_t\}_{t=1}^T$ are computed, the posterior means are obtained by normalising with the precision path from Corollary 1: $\mu_t = \Lambda_t^{-1} \eta_t$. \square

E. Additional Empirical Results

E.1. Ablation on the Importance of Process Noise Parameter

We conduct an ablation study motivated by the theoretical efficiency of fixing the process noise parameter $p_t = 0$ and the observation operator k_t . Under these constraints, the system reduces to a linear time-invariant (LTI) model that can be computed via convolution and unrolled in $\mathcal{O}(\log T)$ time using FFT (see Theorem 3). This ablation investigates whether such computational advantages translate to practical benefits.

Figure 10 compares KLA with learnable process noise against a variant where process noise is fixed to zero (deterministic dynamics, but retaining observation variance $(\Lambda^v)^{-1}$). The results show that removing process noise leads to significantly worse performance across all MADLAB tasks, with accuracy degrading by an average of 49.8 percentage points. The degradation is particularly severe on memorisation (93.6% drop) and in-context recall tasks (54.7% drop), while selective copying shows the smallest decline (18.7% drop).

These empirical findings suggest that process noise is crucial for maintaining model performance, despite the computational overhead of the full Kalman filter formulation. A theoretical investigation of the stability properties of the system, particularly regarding Riccati controllability and observability, and the role of p_t in system stabilisation, represents an interesting direction for future work.

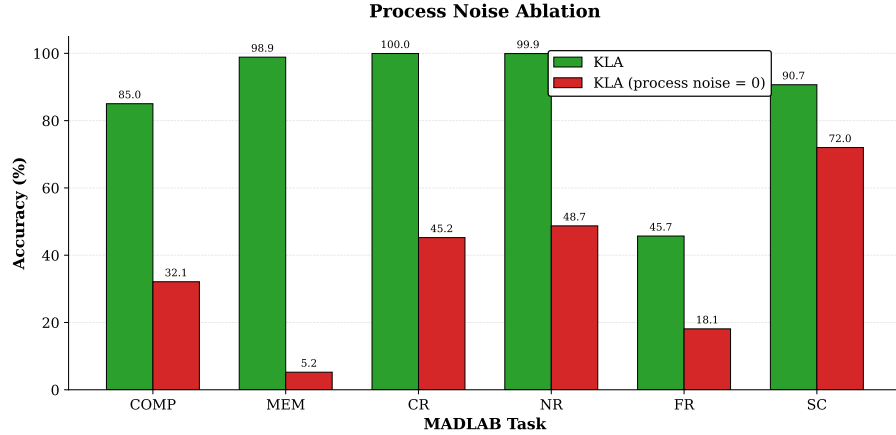


Figure 10. Process noise ablation on MADLAB tasks. Comparison of KLA with learnable process noise versus a variant with process noise fixed to zero ($p_t = 0$). Removing process noise leads to severe performance degradation, with an average accuracy drop of 49.8 percentage points.

E.2. Runtime Scaling

Setup. We benchmark forward-only runtimes for three KLA implementations: a recurrent (time-stepped) Kalman update, the built-in Torch associative scan, and a custom Triton associative scan kernel. All measurements use Torch 2.9.1 on an NVIDIA A100 (80GB), hidden size 960, and float32 precision. The forward-only pass uses a batch size of 1, simulating test-time prompt processing for a 182 million parameter model—critical for deploying sequence models in production settings.

Results. Figure 11 shows that the scan-based implementations scale efficiently with sequence length compared to the recurrent counterparts. These results confirm that information-form filtering can be implemented with the same scan-parallel profile as modern SSM/GLA-style mixers, making KLA practical for long-context prompt processing.

E.3. Equivalent Attention Matrix

As shown in Theorem 2, the information-mean recurrence $\eta_t = f_t \eta_{t-1} + k_t \Lambda_t^v v_t$ (Equation (19)) can be unrolled into a lower-triangular attention matrix \mathbf{W} whose entries are products of **history-dependent forget gates** f_s , keys k_j , and **observation precisions** Λ_j^v . Folding in the output readout query \mathbf{q} and posterior precision scaling $\boldsymbol{\lambda}^{-1}$ gives the full per-channel sequence transformation $\mathbf{M}_{\text{seq}} = \text{diag}(\mathbf{q} \odot \boldsymbol{\lambda}^{-1}) \mathbf{W}$, so that $\mathbf{y} = \mathbf{M}_{\text{seq}} \mathbf{v}$ (plus init-state terms). Figure 12 visualises this two-step structure.

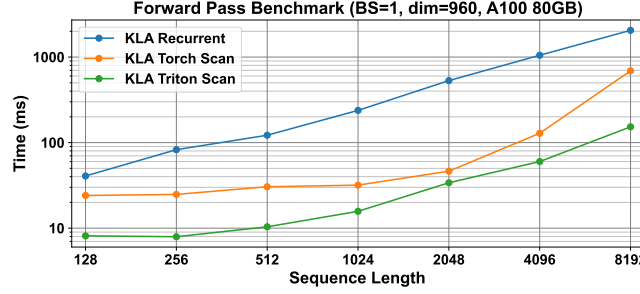


Figure 11. Forward pass (prompt processing) runtime scaling. Wall-clock runtime of KLA implementations across sequence lengths during forward-only pass. Torch Scan uses `torch._higher_order_ops.associative_scan`; Triton Scan uses custom forward kernels.

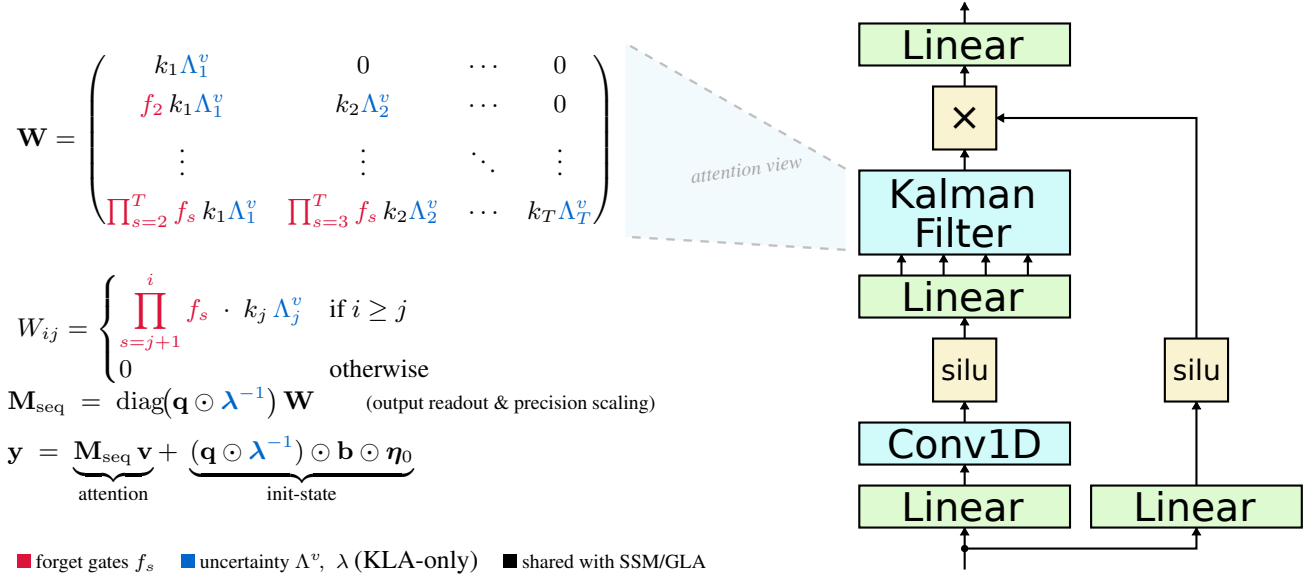


Figure 12. Block architecture and equivalent attention form. Left: The block architecture follows the fused-MLP design of Mamba, with the Kalman Filter as a drop-in replacement for any SSM/Attention primitive. Right: Unrolling the information-mean recurrence (Equation 19): $\eta_t = f_t \eta_{t-1} + k_t \Lambda_t^v v_t$ yields a lower-triangular matrix \mathbf{W} whose entries are products of **history-dependent forget gates** f_s , keys k_j , and **observation precisions** Λ_j^v . Applying the output readout query q_i and **posterior precision** λ_i^{-1} gives the full sequence transformation $\mathbf{M}_{\text{seq}} = \text{diag}(\mathbf{q} \odot \boldsymbol{\lambda}^{-1}) \mathbf{W}$ —the precision terms being unique to KLA and absent in standard SSMs/GLA.

E.4. Kalman Attention Map Visualisation

Unrolling the information-mean recurrence equation 19 yields the lower-triangular matrix \mathbf{W} described in Section E.3; folding in the readout query \mathbf{q}_t and precision scaling $\boldsymbol{\lambda}^{-1}$ gives the per-channel sequence transformation $\mathbf{M}_{\text{seq}} = \text{diag}(\mathbf{q} \odot \boldsymbol{\lambda}^{-1}) \mathbf{W}$ (cf. Figure 12). Because \mathbf{M}_{seq} is lower-triangular, it has the same causal structure as a standard attention matrix; we therefore call it the *Kalman Attention Matrix*.

Figures 13 to 15 visualise the Kalman attention patterns learned by KLA on three MADLAB tasks, each showing four randomly chosen channels. The attention weight at position (t, s) reflects how much the posterior mean at step t is influenced by the observation at step s , weighted by the learned precision ratio.

These visualisations demonstrate that KLA learns task-appropriate attention patterns: selective retrieval for copying tasks, channel specialisation for recall, and uniform retention for memorization—all while maintaining the causal structure inherent to the Kalman filter formulation.

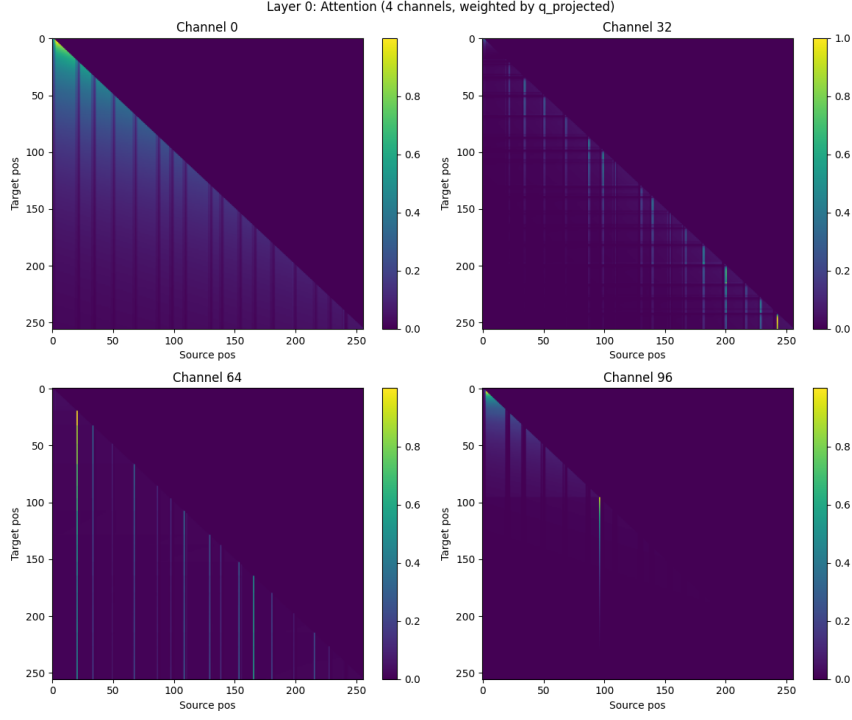


Figure 13. Attention maps for **Selective Copying** (sequence length 256). The model learns sparse, intermittent vertical bands, attending strongly to a small set of task-relevant positions (mostly copy positions). They either activate or suppress these relevant positions. Differences across channels indicate channel-level specialisation in which positions are retrieved.

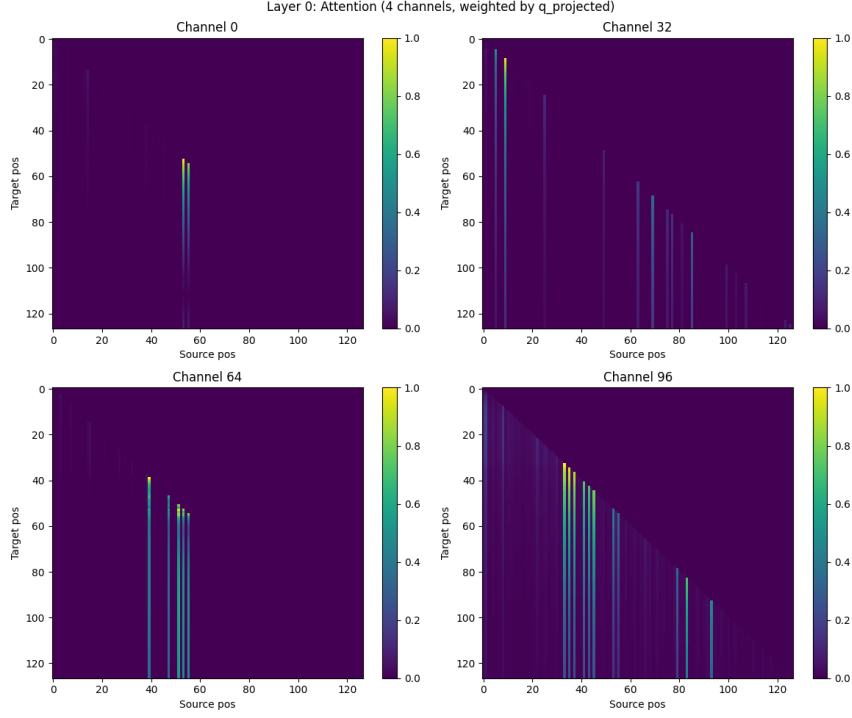


Figure 14. Attention maps for **In-Context Recall** (sequence length 128). The patterns are sparse and “pointer-like”: within each channel, attention concentrates on a small set of source positions (vertical bands) across many target steps, with a mostly low-activation background. Channels show specialisation trends.

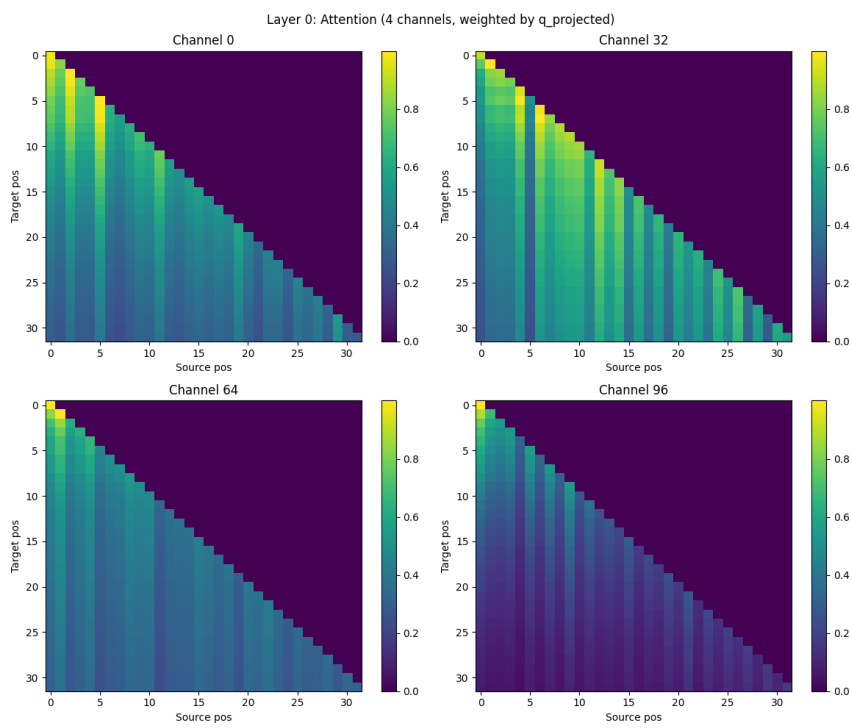


Figure 15. Attention maps for **Memorization** (sequence length 32). The smoother, more gradual decay reflects the task’s requirement to maintain information uniformly across the sequence. All channels show similar patterns, indicating that memorization benefits from redundant, distributed storage rather than selective attention.

Table 5. Mapping from language skills/capabilities to the synthetic probe tasks. Green \checkmark indicates the primary probes/tasks for these skills.

Language Skill / Capability	In-context (MQAR)	Fuzzy Recall	Noisy Recall	Selective Copy	Compression	Memorization
Prompt-level associative retrieval & in-context learning (bindings, multi-query, remapping, basic composition)	\checkmark	\checkmark	\checkmark	\checkmark	\times	\times
Selective attention & noise robustness (noise filtering, long-context stability, calibration)	\times	\times	\checkmark	\checkmark	\times	\times
Ordered copying & pointer-like control flow (order-sensitive working memory)	\times	\times	\times	\checkmark	\times	\times
Information aggregation/bottlenecking (token concatenation for downstream decoding)	\times	\times	\times	\times	\checkmark	\times
Parametric memory of stable facts (weight-based knowledge)	\times	\times	\times	\times	\times	\checkmark

F. Datasets and Benchmarks Used

F.1. MAD LM Suite

To evaluate KLA as a language-modelling primitive, we use a standardised suite of six discrete token manipulation tasks. We adopt the MAD framework (Poli et al., 2024), which consolidates synthetic tasks from prior work into a common specification of data generation, splits, and evaluation. Each task probes a distinct capability (associative retrieval, span compositionality, noise robustness, ordered copying, single-token information aggregation, and parametric memory), allowing us to disentangle model strengths and weaknesses across language skills (see Table 5).

We use the baseline configuration from the MAD framework for all six tasks. Table 6 summarises the key parameters for each task.

Table 6. Baseline configurations for the six MAD tasks used in our experiments.

Parameter	In-context (MQAR)	Fuzzy Recall	Noisy Recall	Selective Copy	Compression	Memorization
Vocab size	16	16	16	16	16	256
Training seqs	12,800	12,800	12,800	12,800	12,800	256
Sequence length	128	128	128	256	32	32
Noise tokens (%)	–	–	20%	–	–	–
Key/value split	8/8	8/8	8/8	–	–	128/128

Additional task-specific settings: Selective Copy (SC) uses `num_copy=16`; In-Context Recall (CR) and Fuzzy Recall (FR) use `multi_query=True`; FR uses motif sizes $k = v = 3$; Noisy Recall (NR) uses `noise_vocab=16` with noise fraction 0.2.

F.1.1. TASK DESCRIPTIONS

In-context recall (MQAR). Sequences consist of key-value pairs with separate vocabularies. The model must predict values for keys that appeared earlier in the sequence. Key-value mappings are randomly shuffled between sequences, forcing the model to learn in-context rather than memorising fixed associations.

Fuzzy in-context recall. An extension of in-context recall where keys and values are represented by variable-length spans (1–3 tokens). This tests the model’s ability to handle compositional keys and maintain associations across multi-token representations.

Noisy in-context recall. Similar to in-context recall, but with 20% of tokens from a separate noise vocabulary randomly inserted. This evaluates the model’s robustness to irrelevant information and selective attention capabilities.

Selective copying. Sequences contain random tokens interspersed with special [blank] and [insert] tokens. The model must copy non-special tokens to [insert] positions in order, while learning to ignore tokens near [blank] markers. This tests selective memorisation and order-preserving working memory.

Compression. Sequences of random tokens ending with a compression token [c]. The model must compress all sequence information into the representation at the compression token position, such that a fixed two-layer MLP can reconstruct any input token given the compressed representation plus a positional encoding.

Memorization. A fixed key-value dictionary is used across all sequences. In each sequence, keys appear with their values masked by [insert] tokens. The model must learn the fixed mappings from the training data, as values never appear in the input during training.

F.1.2. STANDARD TRAINING SETUP IN MAD FRAMEWORK

All tasks use the same architectural scaffolding and training procedure. Training hyperparameters are detailed in Section G.

For most tasks, the training objective is standard next-token prediction via log likelihood (cross-entropy loss). The **Compression** task uses a different setup: the model’s output at the compression token position is passed through a separate two-layer MLP decoder (dimensions [240, 120]) along with a positional encoding to reconstruct each token in the sequence. During training, the model learns to compress the entire sequence into a single representation that enables accurate reconstruction.

All models use a single-layer architecture with a model dimension $d_{\text{model}} = 128$ and an effective state size of 2048.

F.2. Long-Context MQAR

Table 7 lists the data configuration for the long-context MQAR benchmark task (Arora et al., 2023).

Table 7. Long-Context MQAR data parameters.

Long-Context Multi-Query Associative Recall (MQAR)				
Setting	Seq. length	Vocab size	Training seqs	Eval seqs
CR (hard)	2,048	256	12,800	1,280

G. Implementation Details

G.1. Experimental Protocol

Statistical significance. We report results averaged over 5 random seeds to ensure statistical reliability. All comparisons between models use the same random seeds to ensure fairness. For all tasks, we report the mean performance across seeds. For the A5 state tracking task, we consider a task solved if the model achieves $\geq 90\%$ accuracy in at least one of the five seeds.

Open-source code. A minimal anonymous version of the code is attached as a supplementary zip file. The complete implementation, including all custom kernels and experimental code, will be made publicly available upon publication to facilitate reproducibility and future research.

G.2. Training Hyperparameters

We use default settings unless specifically stated otherwise. Table 8 lists the training configuration used across all experiments.

Table 8. Training Hyperparameters (fixed across all models and tasks)

Hyperparameter	Value
Optimizer	AdamW
Learning rate	1×10^{-3}
Learning rate schedule	None
Maximum epochs	750
Early stopping patience	70 epochs
Gradient clipping	5.0
Weight decay	0.0
Precision	32-bit float

KLA-specific settings: We use encoder MLP hidden dimension = 120, decoder MLP dimensions = [240, 120], process noise scale $p = 0.01$ (initial value), discretisation timestep range $\Delta_t \in [0.001, 0.1]$, causal convolution kernel size = 4, and Monte Carlo samples = 10 (used for KLA probabilistic decoding; see Section 5.3).

G.3. MAD-Lab Hyperparameters

To ensure fair comparison, all models are configured with equal effective state sizes by adjusting architecture-specific expansion parameters. For each model dimension, we match the total number of parameters used for state representation across architectures. Note that GatedDeltaNet does not allow exact state-size matching due to constraints on the minimum number of heads and the requirement that expanded key and value dimensions be multiples of 16 or 32. Hence, we assign GatedDeltaNet the next-largest feasible value compared to the other baselines. Table 9 shows the dimensional configuration for each architecture.

Table 9. Model Dimensions (configured for equal state size $S = 2048$)

Model	# Blocks	d_{model}	d_{state}	Other	S
KLA (Ours)	1	128	8	expand=1	2048
Mamba	1	128	16	expand=1	2048
GatedDeltaNet	1	128	-	$e_k=0.5, e_v=1.0, H=4$	2048
GLA	1	128	-	$e_k=0.5, e_v=1.0, H=4$	2048
mLSTM	1	128	-	$H=16, \text{proj_factor}=2.0$	2048

Batch size: We use a batch size of 172 for all MAD-Lab experiments.

G.4. MQAR Hyperparameters

For the MQAR (hard) experiments, we evaluate across three model dimensions with equal state sizes per dimension. All models use 2 layers (repeated blocks). As in the MAD-Lab setup, GatedDeltaNet is given the nearest feasible configuration (see above). Table 10 lists the configuration for each architecture at each dimension.

Table 10. MQAR Model Configurations (state-matched per dimension)

Model	# Blocks	d_{model}	d_{state}	Other	State Size
$d = 64$ (batch size = 64)					
KLA	2	64	16	expand=1	2,048
Mamba	2	64	16	expand=2	2,048
GatedDeltaNet	2	64	-	$e_k=0.75, e_v=1.5, H=2$	2,304
GLA	2	64	-	$e_k=1.0, e_v=1.0, H=4$	2,048
$d = 128$ (batch size = 32)					
KLA	2	128	16	expand=1	4,096
Mamba	2	128	16	expand=2	4,096
GatedDeltaNet	2	128	-	$e_k=0.75, e_v=1.5, H=4$	4,608
GLA	2	128	-	$e_k=0.5, e_v=1.0, H=4$	4,096
$d = 256$ (batch size = 16)					
KLA	2	256	16	expand=1	8,192
Mamba	2	256	16	expand=2	8,192
GatedDeltaNet	2	256	-	$e_k=0.75, e_v=1.5, H=8$	9,216
GLA	2	256	-	$e_k=0.25, e_v=1.0, H=4$	8,192

G.5. A5 State Tracking Hyperparameters

For the A5 state tracking experiments (Section 5.5), we use $d_{\text{model}} = 1024$ and $d_{\text{state}} = 16$ for KLA. We train for up to 500 epochs with early stopping (patience 50), and a learning rate of 3×10^{-4} , and we evaluate over 5 seeds. Values for the baselines are reported as in [Merrill et al. \(2024\)](#).